Research Square

Preprints are preliminary reports that have not undergone peer review.
They should not be considered conclusive, used to inform clinical practice,
or referenced by the media as validated information.

Neuroprotective effect of curcumin against reserpine-induced oxidative damage in the cerebellum of mice in an acute model of Parkinson's disease: Combined in vivo study, molecular docking and molecular dynamics

Mjid Oukhrib

mjid.oukhrib@gmail.com

Cadi Ayyad University

Lahcen Tamegart

Université Ibn Zohr

Lamia Hejji

Abdelmalek Essaâdi University

Hafida El Ghachi

Cadi Ayyad University

Meriem Khedraoui

Hassan II University of Casablanca

Ahmed Draoui

Cadi Ayyad University

Mohammed Haida

Cadi Ayyad University

Imad Hammoudan

Sidi Mohamed Ben Abdallah University

Samir Chtita

Hassan II University of Casablanca

Halima Gamrani

Cadi Ayyad University

Mohamed Chraa

Cadi Ayyad University

Research Article

Keywords: Parkinson's Disease, Curcumin, Oxidative Damage, cerebellum, Molecular docking, Molecular dynamics simulation

Posted Date: September 21st, 2026

DOI: https://doi.org/10.21203/rs.3.rs-10974731/v1

License: This work is licensed under a Creative Commons Attribution 4.0 International License.
Read Full License

Additional Declarations: No competing interests reported.

Neuroprotective effect of curcumin against reserpine-induced oxidative damage in the cerebellum of mice in an acute model of Parkinson's disease: Combined in vivo study, molecular docking and molecular dynamics

Mjid Oukhrib[a], Lahcen Tamegart[a,b,*], Lamia Hejji[c], Hafida El Ghachi[a], Meriem Khedraoui[d], Ahmed Draoui[a], Mohammed Haida[e], Imad Hammoudan[f], Samir Chtita[d], Halima Gamrani[a,1] and Mohamed Chraa[a,1]

[a]Neurosciences, Pharmacology and Environment Team, Faculty of Science Semlalia, Laboratory of Clinical, Experimental and Environmental Neurosciences, Faculty of Medicine and Pharmacy, Cadi Ayyad University, Marrakech, Morocco.

[b]Biology, Ecology and Health Laboratory, Department of Biology, Faculty of Science, Abdelmalek Essaadi University, Tetouan, Morocco.

[c]Department of Chemistry, Faculty of Science, University of Abdelmalek Essaadi, B.P. 2121, M'H IannechI, 93002, Tetouan, Morocco

[d]Laboratory of Analytical and Molecular Chemistry, Faculty of Sciences Ben M'Sik, Hassan II University of Casablanca, P. O. Box 7955, Casablanca, Morocco

[e]Water, Biodiversity, and Climate Change Laboratory, Faculty of Sciences Semlalia, Cadi Ayyad University,Marrakech, Morocco.

[f]LIMAS, Department of Chemistry, Faculty of Sciences Dhar El Mahraz, Sidi Mohamed Ben Abdallah University, Fez 30000, Morocco

Abstract

The neuroprotective potential of curcumin was studied in a reserpine-induced model of progressive Parkinsonism in mice. Male Swiss mice were given daily doses of curcumin-III (30 mg/kg b.w), Madopar (120 mg/kg b.w), or a combination of the two substances, plus three doses of reserpine (0.25 mg/kg b.w) spaced 48 hours apart. Motor behaviour was assessed after the last treatment. Histopathological examinations, indicators of oxidative stress, and neuroinflammation were evaluated at the end of treatment. Treatment with curcumin prevented cell damage in the Purkinje cells of the cerebellum and reduced their oxidative state index. As a result, curcumin reduced motor deficiencies in a progressive animal model of Parkinson's disease, most probably due to an antioxidant action. Also, our comparative study revealed that curcumin binding interactions with Catechol-O-MethylTransferase were stronger than those of the Madopar and thirteen van der Waals interactions (Asp141, Asn170, Glu199, Trp38, Pro174, Tyr68, Gly66, Ala67, Glu90, Ser119, Arg146, Gln120 and Ala118) ensured the formation of the Catechol-O-MethylTransferase -Curcumin complex.

Keywords: Parkinson's Disease; Curcumin; Oxidative Damage; cerebellum; Molecular docking; Molecular dynamics simulation.

***Corresponding author: l.tamegart@uae.ac.ma (L.Tamegart)**

[1]Both authors contributed equally to this work.

1. Introduction

Parkinson's disease (PD) is a chronic neurological condition that is both incurable and progressive, making it one of the most difficult diseases to treat (Prajjwal et al., 2024). It is the second most common neurological condition in older people, after Alzheimer's disease, affecting around 6.3 million people over the age of 65 (Chopade et al., 2023). PD is characterized by the degeneration or death of dopaminergic neurons in the substantia nigra, as well as the formation of Lewy bodies, clusters of proteins containing alpha-synuclein, in surviving neurons in the nervous system (Regoni et al., 2024). It has been associated with motor dysfunction, including rigidity, resting tremors, and postural instability (Pasquini et al., 2023). Non-motor symptoms of PD include problems with the autonomic system and neuropsychiatric symptoms such as depression and anxiety, which can increase morbidity (Qamar et al., 2024). The loss of dopaminergic cells in PD is mainly caused by pathogenic processes such as neuroinflammation and oxidative stress (Dhiman et al., 2024).

Reserpine (RES) can produce motor disorders similar to those of PD, such as limb stiffness, hypokinesia, akinesia, catalepsy, and mouth tremors (Juza et al., 2023). Blockade of vesicular monoamine transporters 1 and 2 (VMAT1 and 2) leads to a reduction in the release of monoamines into the synaptic cleft and their accumulation in the cell, as well as an overproduction of free radicals during neurotransmitter metabolism, causing oxidative damage and the appearance of motor symptoms(Juza et al., 2023).

Mitochondrial dysfunction, α-synuclein aggregation, and oxidative stress have been linked to the aetiology of neurodegenerative diseases such as Parkinson's (Afsheen et al., 2024).Among them, oxidative stress develops following a dysregulation of the cellular redox system, which occurs when the creation of reactive oxygen species exceeds clearance by cellular antioxidant enzymes and chaperone molecules (Orfali et al., 2024). Importantly, when the degree of reactive oxygen species (ROS) generation increases and a redox imbalance occurs, oxidative stress becomes pathogenic (Kishi et al., 2024). Post-mortem investigations have revealed elevated levels of Thiobarbituric Acid Reactive Susbtances (TBARS) in the plasma and substantia nigra of Parkinson's patients (Hassani & Esmaeili, 2024).

The cerebellum is a motor coordination centre, and any alteration to it leads to motor deficiencies and cerebellar ataxia (Iskusnykh et al., 2024). Pathological alterations in the cerebellum have been observed in humans with PD and in animal models (Turkez et al., 2023). In an MPTP animal model, neuronal degeneration was observed in the cerebellum and

characterised by the loss of Nissl-stained Purkinje cells and an increased number of recurrent MPTP injections (Ge et al., 2024). A recent study showed that sustained hyperactivation of Purkinje cells in monkeys with chronic PD corresponded to the degree of dopaminergic neuronal loss in the substantia nigra (Heman et al., 2012).

Curcumin (CUR) is a natural polyphenolic antioxidant molecule extracted from the root of the perennial herb Curcuma longa, widely known as turmeric and long used in traditional Asian medicine (Goel et al., 2008; Lodha & Bagga, 2000; Srimal & Dhawan, 1973). Turmeric has been used for thousands of years in India as a food preservative and as a treatment for human diseases caused by inflammation and injury (Tobinai et al., 1992; Uozumi et al., 1995). Some research suggests that CUR may reduce the prevalence of PD. An epidemiological study has shown that Indian communities that regularly consume CUR have fewer age-related alterations in the dopaminergic neurons of the substantia nigra (Darvesh et al., 2012). CUR can cross the blood-brain barrier and act as an antioxidant and anti-inflammatory agent, making it potentially effective in the treatment of neurodegenerative diseases such as Parkinson's and Alzheimer's (Giri et al., 2004). CUR is therefore a natural antioxidant that could be beneficial in the treatment of PD.

The present study aimed to evaluate the effects of CUR on motor changes, cerebellar oxidative stress, and tissue damage in PD induced by the administration of RES in mice. The possible modulation of the action of the anti-parkinsonian drug Madopar by CUR was also studied. In addition, to inhibit COMT enzyme and dopamine metabolism and then stop the PD progression.

2. Materials and methods

2.1. Chemicals

Reserpine crystallized (99%),7-bis(4-hydroxyphenyl) hepta-1,6-diene-3,5- dione (, Dimethylsulfoxide (DMSO, 99.9%) were obtained from Sigma-Aldrish (Madrid, Spain Anti Glial Fibrillary Acidic Protein (Anti-GFAP: DAKO, monoclonal mouse anti-human GFAP, lot#00072911, ref#M0761).NaCl, ethanol, tetrazolium nitro blue, phosphate buffer, methionine, riboflavin, thiobarbituric acid reactive, malonaldehyde, formalin, paraffin block, thin ribbons, hematoxylin, eosin, urethane anesthesia, transcardiac perfusion, paraformaldehyde, phosphate-buffered saline, Polyethylene glycol (PEG), bovine serum albumin, Triton, monoclonal anti-glial fibrillary acidic protein (GFAP) antibody, diluted 1:1000 in PBS (0.1M, pH7.4), Triton (0.3%), and BSA (1%). A secondary antibody (anti-rabbit

immunoglobulin, 1/500) was used to detect immunoreactivity for 2 hours at room temperature. The sections were then collected and mounted in Eukit (Sigma-Aldrich, Buchs, Switzerland) after dehydration for light microscopy. These tests showed that the primary antibody used against GFAP showed specific labeling as previously published.

2.2.Animals

Adult male Swiss mice, 12 to 15 weeks old and weighing 30 ± 3 g were obtained from the central animal house of Cadi Ayyad University of Marrakech (UCAM), Morocco. Animals were maintained in polycarbonate cages in a temperature-controlled room (25 ± 2 °C) with a 12-hour light/dark cycle (lights on at 7 am). Food and water were provided *ad libitum*. All experiments were performed according to the guidelines of UCAM. All animals were treated in compliance with the European Regulation on the ethical evaluation and authorization of projects involving the use of animals in experimental procedures, which went into effect on 1 February 2013. Every attempt was made to decrease the number of animals utilized and the pain they experienced.

2.3.Experimental design and treatment

Swiss male mice aged 12-14 weeks (30 ± 3 g) were randomly assigned to the following groups: (1) Control (CTR), RES vehicle (0.9% NaCl +5% DMSO subcutaneously), (2) RES alone (RES) (da Silva Córneo et al., 2020; Oukhrib et al., 2023), (3) RES+CUR-III dissolved in olive oil (30 mg/kgb.w, RES+CUR) (Tamegart et al., 2021), (4) RES+ Madopar dissolved in saline 0. 9% (120 mg/kg b.w, RES+MAD) and (5) RES+CUR-III +Madopar combination (30 mg/kg b.w, 120 mg/kg b.w, respectively, RES+CUR-MAD). All groups, except the CTR group, received three injections of RES at a concentration of 0.25 mg/kg subcutaneously at 48-hour intervals (days 1, 3, and 5) (da Silva Córneo et al., 2020; Oukhrib et al., 2023). The treated groups received their treatment orally, daily for five days, two hours before the RES injection (**Fig. 1**).

2.4.Behavioural and biochemical analysis

2.4.1. Open Field and Rotarod tests

To assess the locomotor activity of our animals, we used the "open field" test. Twelve hours after completing the 5-day treatment, each animal was placed in the middle of the field and allowed to explore freely for 5 min. The animal's movements are filmed by a video camera placed on top of the open field. The videos were subsequently analysed using tracking software. Standard parameters of locomotor activity, such as ambulatory distance, average speed,

exploratory behaviour, time spent in the centre, and time spent in the margins, were recorded. Once the tests were completed, the mice were returned to their original cages and the open field device was cleaned with 70% ethanol to eliminate traces left by the previous animal (urine, excrement) that could influence the next animal (Broadhurst & London, 1960; Cordaro et al., 2018; Harrington, 1972; Paterniti et al., 2017).

The Rotarod test was adapted to assess the motor coordination of the animals. The device had a rotating rod and was divided into five compartments, allowing five mice to be tested at a time. All animals were trained on the Rotarod 24 hours prior. Each mouse was placed on the rotating rod with the speed of rotation set at 15 rotations per minute, and the mice were tested for a maximum of 300 seconds. Using a mechanical fall detector and a timer for each lane, the device automatically records the time when a mouse falls off the rotating rod. The time spent on the rod was recorded for each mouse and used as a measure of fall duration. The test and training were performed during the day, between 12:00 and 14:00 (Cordaro et al., 2018; Monville et al., 2006; Paterniti et al., 2017).

2.4.2. Biochemical analysis of superoxide dismutase activity and Malondialdehyde

Mice were sacrificed by cervical decapitation approximately 12 hours after behavioural testing to perform biochemical tests. Brains were rapidly collected and cleaned with ice-cold saline before the cerebellum was dissected. Isolated samples from the cerebellum were immediately processed to determine parameters related to oxidative stress.

The superoxide dismutase activity was determined by measuring the inhibition of photochemical reduction of tetrazolium nitro blue, with some modifications (Oukhrib et al., 2023). A 3-mL reaction mixture contained 100 mM phosphate buffer (pH 7.8), 55 mM methionine, 0.75 mM tetrazolium nitro blue, 0.1 mM riboflavin, and 50µL of the enzyme extract. After the addition of riboflavin, the reaction was initiated by placing the tubes under 20-W fluorescent lamps at 25◦C. The absorbance was read after 15 min at 560 nm (Beyer & Fridovich, 1987). The lipid peroxidation was determined by measuring thiobarbituric acid reactive substance in terms of malondialdehyde, which gave a pink-colored molecule. The absorbance at 548 nm was used to determine the pink-colored product. The outcome was represented in nmol malondialdehyde/mg protein (Oukhrib et al., 2023).

2.5. Histological analysis

After animal sacrifice, brain samples were extracted and preserved in 10% formalin for 24 hours. The samples were then dehydrated using baths with increasing concentrations of ethanol

ranging from 50% to 100%. Using a semi-automatic microtome (Leica Biosystems RM 2245), the paraffin block containing the tissue was segmented into thin ribbons (4µm thick). The sections were stained with hematoxylin and eosin.

2.6. Immunohistochemistry of GFAP

Mice were sacrificed 12 hours after behavioral testing; urethane anesthesia (40 mg/kg i.p.) was provided, followed by transcardiac perfusion with saline (0.9% NaCl) and paraformaldehyde (4%) in phosphate-buffered saline (PBS, 0.1 M, pH 7.5). Brains were post-fixed in the same solution overnight at 4°C after collection. Dehydration in alcohol was followed by inclusion in Polyethylene glycol (PEG). Coronal sections through the cerebellum were cut 20 µm thick with a microtome (Leica Biosystems RM 2245) and collected in PBS. In a solution of PBS containing 0.1% bovine serum albumin (BSA) and 0.3% triton, the selected sections were incubated for 2 hours and then overnight at 4°C with the monoclonal anti-glial fibrillary acidic protein (GFAP) antibody, diluted 1:1000 in PBS (0.1M, pH7.4), Triton (0.3%), and BSA (1%). A secondary antibody (anti-rabbit immunoglobulin, 1/500) was used to detect immunoreactivity for 2 hours at room temperature. The sections were then collected and mounted in Eukit (Sigma-Aldrich, Buchs, Switzerland) after dehydration for light microscopy. These tests showed that the primary antibody used against GFAP showed specific labeling as previously published (Draoui et al., 2019).

2.7. Immunolabelling quantification

We utilized ImageJ software to quantify GFAP staining immunohistochemically. Cerebellum sections from different animals in each group were utilized for GFAP immunoreactivity. After converting each image to binary mode, the percentages of black pixels were calculated using the image's histogram option. The study employed three randomly selected parts per animal from each group as samples.

2.8. Molecular docking and molecular dynamics simulation

Molecular docking is a crucial technique for exploring the types of interactions that can form when a compound binds to a protein and for calculating the free energy associated with their binding. The original 3D structural configuration of the protein catechol O-methyltransferase (COMT), PDB: 1H1D, was obtained from the Protein Data Bank (www.rcsb.org) (Bonifácio et al., 2002). We carried out its preparation using an Autodock tool program (Morris et al., 2009), removing unwanted ligands and cofactors after adding polar hydrogen atoms, Gsteiger and Kolleman atomic charges, as well as missing residues. Then, the

active site is determined by the location of the crystallized co-ligand. The PDB protein file was then converted to pdbqt format to make it suitable for molecular docking. Curcumin and Madopar were downloaded from the PubChem database server in SDF format, then converted to PDBQT format. Afterward, we docked them with their proteins using Auto Dock Vina software(Trott & Olson, 2010). Finally, the 2D intermolecular interactions of the candidate protein-drug complexes were visualized using Discovery Studio software (Studio, 2016).

The binding affinity of the curcumin compound and the reference drug at the target active site was determined by molecular dynamics simulation (MDs) in accordance with our previous work (Abchir et al., 2023; Chalkha et al., 2022; Daoui et al., 2022; Yamari et al., 2023). A 100 ns simulation was carried out in the Maestro-Desmond software. The protein-ligand complex was placed in the center of a cubic box with a size of 15 Å. TIP3P water molecules (Mark & Nilsson, 2001) were added, along with appropriate ions such as 0.15 M salt, which were randomly distributed into the solvent system to neutralize the medium. The system was parameterized using the OPLS3e force field constants from the Desmond package (Roos et al., 2019). MDs of the production were conducted with NPT set at 298 K and 1 bar. Trajectories of the root mean square deviation (RMSD) and (RMSF), protein-ligand contacts (PL), solvent accessible surface area value (SASA), radius of gyration value (Rg), MolSA, and the polar surface (PSA) were generated to study the stability of the protein-ligand complex. Finally, the free energies of protein-candidate or drug bindings were calculated at 50 ns of simulation, using the MM-GBSA method via the Prime module of Maestro to further confirm the results.

2.9. Statistical analysis

Using one-way analysis of variance (ANOVA), the statistical significance of differences between groups was assessed. Tukey's test was used to examine post hoc differences in group means. Data are expressed as mean S.E.M., and $p<0,05$ indicates a statistically significant difference. For statistical analysis, SPSS 10.0 software for Windows (SPSS, IBM, Chicago, IL, USA) was used.

3. Results and Discussion

3.1. Effect of reserpine, Madopar and curcumin-III on motricity and antioxidant activity

3.1.1. Rotarod test

The use of the rotarod test after the last treatment showed a significant reduction in motor coordination and balance ($p<0.05$) observed in the group treated with RES alone, represented

by the latency time on the rotarod axis compared to the control group. Similar to the baseline treatment (Madopar), CUR treatment was able to significantly restore the latency time on the rotarod axis ($p<0.05$). The co-treatment with CUR and Madopar treatment was also able to suppress the damage induced by RES treatment significantly($p<0.05$) (**Fig. 2A**).

Reserpine was one of the first animal models of PD. RES is an alkaloid extracted from the plant *Rauwolfia serpentina*. It is an irreversible inhibitor of VMAT1 and 2 (Leão et al., 2015; Vergo et al., 2007). As a neurotoxicant, it prevents VMAT function by inhibiting the uptake and transport of monoamines into vesicles present in presynaptic neuronal terminals (Lobay, 2015). This procedure reduces the release of monoamines into the synaptic cleft and their accumulation in the cell. Due to the excess of free radicals created during the metabolism of these neurotransmitters, oxidative stress increases (Bilska et al., 2007; da Silva Córneo et al., 2020; Fuentes et al., 2007; Leão et al., 2015b; Lobay, 2015; Oukhrib et al., 2023). The RES model reproduces the main features of PD symptomatology, neurochemistry, and pharmacology.

3.1.2. Open field test

Our results show that RES induced a significant decrease ($p<0.05$) in locomotor activity represented by the distance covered by the animals during five minutes (**Fig. 2B**). The treatment with CUR induced a significant ($p<0.05$) restoration of locomotor activity, compared to animals treated with RES alone. For the reference group RES+MAD, the results showed a significant restoration of locomotor activity compared to the group treated with RES ($p<0.05$). The locomotor activity of the group treated with CUR and the reference treatment increased significantly with respect to the distance covered compared to the group treated with RES only (**Fig. 2B**).

Acute injection of a low dose of RES in mice has been shown to cause motor deficits. These impairments include a decrease in motor activity, as evidenced by a decrease in free-field distance, and a decrease in motor coordination, as evidenced by a decrease in rotational axis latency (Carlsson & Carlsson, 1989; da Silva Córneo et al., 2020b; De Freitas et al., 2016; Oukhrib et al., 2023). According to research conducted by several teams, these behavioural alterations correlate with an increase in lipid peroxidation in several brain areas (V. C. Abílio et al., 2003; Beserra-Filho et al., 2019; da Silva Córneo et al., 2020a; Oukhrib et al., 2023). Furthermore, these alterations are associated with dysregulation of antioxidant enzyme activity (V. Abílio et al., n.d.; da Silva Córneo et al., 2020a; Oukhrib et al., 2023). Consequently, the

animal model shows alterations similar to those observed in patients with PD and is considered an effective approach for evaluating new drugs against PD (Chaudhuri et al., 2006; Draoui et al., 2019; Lopatina et al., 2014; Voon & Fox, 2007).

3.1.3. Oxidative damage and antioxidant system

The level of MDA was significantly decreased ($p< 0.001$) in the cerebellum of treated animals compared to the controls (**Fig. 3A**). The level of SOD increased significantly ($p< 0.01$) in the cerebellum of animals treated with RES alone, while there was a highly significant decrease in enzyme activity in the cerebellum of groups treated with RES plus CUR, MAD or both ($p< 0.001$) (**Fig. 3B**).

CUR has been shown to reduce ROS prevent oxidative cell damage, and exhibit antioxidant, anti-cancer, and anti-inflammatory properties (Aggarwal et al., 2011 ; Kabeer et al., 2019; Maheshwari et al., 2006). Pharmacotherapy with CUR and the co-treatment of CUR and MAD significantly restored the motor activity and coordination impaired by RES, as shown by the results of behavioural tests. This improvement in motor behaviour can be explained by the antioxidant potential of this molecule while protecting the various neuronal systems involved in the motor process. This is in agreement with the results of studies showing that CUR improves motor behaviour in rodents due to its antioxidant potential against various neurotoxic substances that cause oxidative damage in the brain (El-Shamarka et al., 2022a; Hasan et al., 2020; Khadrawy et al., 2021). It is also possible that the improvement brought about by the administration of CUR for the motor deficit induced by RES is the result of the modulation that CUR brings to the various monoaminergic neurotransmission systems, especially dopamine (El-Shamarka et al., 2022a; Hasan et al., 2020; Khadrawy et al., 2021; Mohammed et al., 2019; Ojha et al., 2012). This improvement may also be linked to the reducing power of CUR, which promotes neuroprotection of Purkinje cells in the cerebellar vermis. CUR protected against the increase in oxidative stress generated by RES and reduced the RES-induced inhibition of vesicular monoamine transporters by reducing lipid peroxidation and maintaining stable SOD levels. Our results are consistent with previous research revealing the neuroprotective potential of CUR against the negative consequences of oxidative stress (El-Shamarka et al., 2022b; Khadrawy et al., 2021; Mohammed et al., 2019).

3.2. Histological and immunohistochemical analysis

The H&E staining was used to assess neuronal apoptosis in the cerebellum after exposure to the different treatments. As shown in the figures (**Fig. 4**), the number of degenerated Purkinje

cells was significantly higher in the cerebellum of animals after administration of RES alone than in the cerebellum of control animals ($p<0.001$). Administration of CUR, MAD, or both significantly reduced the rate of Purkinje cell degeneration in the cerebellum ($p<0.001$) (**Fig. 4**).

The cerebellum has been shown to contribute significantly to the coordination, precision, and regulation of body movements by processing sensory information and adjusting muscle activity. In addition, the cerebellum is involved in other behavioural functions, such as emotion and cognition, through a range of neurotransmitters (Khadrawy et al., 2017) , including GABA, which is released by Purkinje neurons in the cerebellum to control and coordinate movement (Bowery et al., 2002). These Purkinje cells ensure communication between the cerebellar cortex and the brainstem and control motor function via GABAergic projections (Chaumont et al., 2013; De Zeeuw & Berrebi, 1995; Person & Nature, 2012; Uusisaari et al., 2008). Pathological alterations of the cerebellum induce tremors, rigidity, and gait problems associated with non-motor symptoms in PD (Khadrawy et al., 2017). Our study showed that treatment with RES led to changes in cerebellar cells. A significant rate of degeneration in Purkinje cells was observed, which may explain the alteration in motor processes (**Fig. 4F**). This degeneration is the result of the accumulation of ROS generated by alterations in neurotransmitter levels following treatment with RES (Khadrawy et al., 2017) .

Astrocyte density and morphology in the cerebellum were assessed using GFAP immunostaining. In addition, we assessed the proportion of the cerebellar region occupied by GFAP immunostaining to account for the effect of CUR on astroglial hypertrophy (**Fig. 5**).

The number of GFAP-positive cells increased in the cerebellum after RES alone, while CUR, MAD, or both only increased slightly. Swelling and deformation in the morphological appearance of astrocytes were observed in the different groups other than the control group and to a greater extent in the group treated with RES alone, as shown in the figure (**Fig. 5**).

Astrocytes are support cells of the nervous system that are responsible for maintaining cerebral homeostasis. At different levels, these cells collaborate with various neuronal systems to facilitate neurotransmitter trafficking and recycling, energy metabolism, ion homeostasis, and defence against oxidative damage (Colombo et al., n.d.; van Deijk et al., 2017) . The astrocyte's ability to accept signals from the synaptic cleft and provide feedback by releasing its signalling molecules is facilitated by its anatomical proximity to the neuron. The discovery of gliotransmitters such as GABA, glutamate, ATP, and D-serine, which are secreted glial

signalling molecules by vesicles within the synaptic cleft, supports this potential (Volterra et al., 2014; Zorec et al., 2016). GFAP immunolabelling showed that treatment with RES triggered astrocyte activation in the cerebellum as demonstrated by increased density, morphological changes, swelling, and deformation. A previous study has shown that oxidative stress induced by RES administration triggers reactive gliosis to protect neurons in their environment from ROS (Draoui et al., 2019; Voronkov et al., 2013).

Treatment with CUR showed neuroprotective effects due to its antioxidant potential. We found that CUR was able to reduce the percentage of Purkinje cells that degenerated because of the oxidative stress generated by the blockade of VMAT-1 and 2. In addition, we reported that CUR can decrease the degree of astrocytic reaction against ROS produced in their microenvironment. These results are in agreement with what has been demonstrated by several studies, Hasan et al., 2019, suggested that treatment with CUR offers effective neuroprotection to Purkinje cells located in the cerebellar vermis against the neurotoxicity of rotenone (Hasan et al., 2020). In studies targeting the effects of CUR on the glial system, this molecule showed intense potential as an anti-inflammatory substance while reducing the levels of inflammatory responses induced by MPTP administration (H. Gao et al., 2003; H. M. Gao et al., 2003; McGeer & McGeer, 2008). Therefore, our study suggests that CUR protects against RES-induced central damage through its antioxidant action.

3.3. Molecular docking and molecular dynamics

Molecular docking analysis revealed that CUR and the reference drug Madopar were linked with the protein COMT via various non-covalent interactions. CUR interacts through a series of hydrophilic and hydrophobic interactions. 2D interactions show that the main source of its bonds is Van der Waals forces, hydrophobic, and electrostatic interactions **(Fig. 6)**. It was observed that thirteen van der Waals interactions (Asp141, Asn170, Glu199, Trp38, Pro174, Tyr68, Gly66, Ala67, Glu90, Ser119, Arg146, Gln120 and Ala118) ensured the formation of the COMT-CUR complex, while the residues HIS142 and TRP143 were involved in hydrophobic bonds. The amino acids Met40, Met91 and Lys144 were included in electrostatic interactions. Madopar was bound in the active site via the establishment of three hydrogen bonds with these residues Asp30, Asp44 and Glu27, and the formation of two electrostatic bonds of Pi-Anion type with these residues Glu27 and Asp44, as well as three hydrophobic bonds of two types Pi-Pi T-shaped, Alkyl with these residues Tyr197, Leu26 and Lys202. The docking scores displayed in **Table 1** reveal that CUR has a binding energy of -8.0 kcal/mol; On

the other hand, the reference drug Madopar showed the lowest binding energy of −7.2 kcal/mol. This indicates that overall, CUR binding interactions were stronger than those of the reference interactions, meaning that the CUR compound had a greater affinity for protein binding than Madopar.

Table 1. Docking scores of Curcumin and Madopar docked complexes.

Ligands	Curcumin	Madopar
Score (kcal/mol)	-8.0	-7.2

The structural stability of the protein-ligand complexes over 100 ns was monitored by several parameters resulting from molecular dynamics. The RMSD curves of the COMT-CUR and COMT-Madopar complexes are shown in **Fig. 7**. The protein COMT in complex with CUR gradually reached a stabilized value of 0.9 Å in 60 ns and afterward deviated to a value of 1.2 Å, remaining stable until the end. Moreover, the RMSD of CUR adjusted to the protein showed a maximum shift of 2.8 Å at the start of the simulation, and after 30 ns, the RMSD lowered to 0.8 Å (**Fig. 7a**). While the RMSD curve of protein COMT in complex with the reference drug Madopar showed fluctuations of 1.05 Å during the 100 ns; On the other hand, the reference exhibited movements of 5.5 Å, remaining stable throughout the simulation with minimal displacements in some nanoseconds **(Fig. 7b)**. Therefore, the COMT-CUR complex is considered more stable due to its lower deviation observed in the RMSD curve (Yamari et al., 2024).

The RMSF trajectory of COMT-CUR shows that all residues exhibit fluctuations smaller than 1.2 Å, as shown in **Fig. 8a**, and the same is observed for COMT-Madopar, as shown in **Fig. 8b**. This indicates that there is no conformational change in the protein caused by the binding of CUR or Madopar, signifying the stability of the two complexes.

The stacked bar histogram in Figure 10 shows that the protein amino acids exhibited various types of interactions with the two compounds, including hydrophobic interactions, hydrogen bonds, and water-bridged hydrogen bonds. **Fig. 9a** shows that CUR is engaged in the active site by the formation of a single hydrogen bond of 100% participation rate with the amino

acid SER119, and hydrophobic contacts MET40, MET91, HIS142, TRP143 and LYS144 with formation rate of 28, 39, 90, 91 and 88% respectively, and also water bridges were observed with these residues TYR95 and TRP143 with occupancy rate of 25 and 28 % respectively. Madopar was linked with the protein through the contact of two hydrogen bonds established by Gln23 and Thr34 in the fraction range of 49 and 78% respectively, and water bridge bonds established by Gln23, Glu27, Asp30, Thr31, Asp44, Tyr71, Arg78 and Tyr200 in the fraction range 30, 22, 22, 18, 25, 15, 23, and 25%, respectively **(Fig. 9b)**.

The stability of the compounds in the binding pocket was demonstrated by analyzing these properties shown in **Fig. 10**. The RMSD of the ligand represents the squared deviation of the compound from its first conformation at time t = 0. The RMSD value for CUR and Madopar is less than 1.2 Å and 3 Å respectively. The Rg values for CUR in the binding pocket were 4.4–5 Å from 0 to 35 ns, and after 35 ns, the Rg remained stable at 4.9 Å until the end of the simulation. The Rg values of Madopar in the same binding pocket were stable at 6.0 Å from 0 ns to 88 ns, then increased to 6.25 Å, and at the end of the simulation returned to its initial stability. The MOLSA plots are associated with a Van Der Waals surface, calculated with a probe radius of 1.4 Å, and the SASA plots measure the accessibility of the solvent to the ligand. Furthermore, the PSA plots are influenced by the nitrogen and oxygen atoms. Analysis of these graphs reveals that CUR shows only minimal fluctuations at 312, 80 and 186 Å^2, and for Madopar at 550, 480 and 130 Å^2. To further verify the quality of MDs, post-MD MM/GBSA calculations were performed for comparison between CUR and the reference. CUR has a binding energy of -60.41 kcal/mol, which is lower than the reference binding energy of 45.49 kcal/mol. Meaning that CUR's inhibitory activity against the protein may prevail over that of Madopar, suggesting that CUR may likely have great potential in treating the disease.

4. Conclusion

Current results suggest that CUR prevents motor disorders in mice in an RES-induced PD model and reduces disruption of the antioxidant system in the cerebellum of mice, providing central protection to various neural systems and reducing histological damage. In addition, molecular docking and molecular dynamics studies were performed to identify the stabilising capacity of CUR and its inhibitory effect on COMT, thereby reducing dopamine metabolism. CUR can therefore be considered a potential therapeutic approach for PD. The mechanism of action and medical applications of this molecule require further study.

Competing Interest Declaration

The authors declare that they have no known competing financial interests or personal relationships that could have appeared to influence the work reported in this paper.

Acknowledgments

This research did not receive any specific grant from funding agencies in the public, commercial, or not-for-profit sectors.

References

Abbaoui, A., & Gamrani, H. (2019). Obvious anxiogenic-like effects of subchronic copper intoxication in rats, outcomes on spatial learning and memory and neuromodulatory potential of curcumin. *Journal of Chemical Neuroanatomy*, *96*, 86–93. https://doi.org/10.1016/J.JCHEMNEU.2019.01.001

Abchir, O., Daoui, O., Nour, H., Yamari, I., Elkhattabi, S., Errougui, A., & Chtita, S. (2023). Exploration of Cannabis constituents as potential candidates against diabetes mellitus disease using molecular docking, dynamics simulations and ADMET investigations. *Scientific African*, *21*, e01745.

Abílio, V. C., Araujo, C. C. S., Bergamo, M., Calvente, P. R. V., D'Almeida, V., Ribeiro, R. D. A., & Frussa-Filho, R. (2003). Vitamin E attenuates reserpine-induced oral dyskinesia and striatal oxidized glutathione/reduced glutathione ratio (GSSG/GSH) enhancement in rats. *Progress in Neuro-Psychopharmacology and Biological Psychiatry*, *27*(1), 109–114. https://doi.org/10.1016/S0278-5846(02)00340-8

Abílio, V., Silva, R., Carvalho, R., & … C. G. (2004). Important role of striatal catalase in aging-and reserpine-induced oral dyskinesia. *Elsevier*. https://www.sciencedirect.com/science/article/pii/S002839080400108X

Afsheen, S., Rehman, A. S., Jamal, A., Khan, N., & Parvez, S. (2024). Understanding Role of Pesticides in Development of Parkinson's Disease: Insights from Drosophila and Rodent Models. *Ageing Research Reviews*, 102340.

Aggarwal, B., sciences, B. S.-T. in pharmacological, & 2009, undefined. (n.d.). Pharmacological basis for the role of curcumin in chronic diseases: an age-old spice with modern targets. *Cell.ComBB Aggarwal, B SungTrends in Pharmacological Sciences, 2009•cell.Com*. Retrieved October 9, 2023, from https://www.cell.com/trends/pharmacological-sciences/fulltext/S0165-6147(08)00252-6?cc=y

Beserra-Filho, J., Macêdo, A. de, & … A. L.-. (2019). Eplingiella fruticosa leaf essential oil complexed with β-cyclodextrin produces a superior neuroprotective and behavioral profile in a mice model of Parkinson's. *Food and Chemical*. https://www.sciencedirect.com/science/article/pii/S0278691518308585

Beyer, W. F., & Fridovich, I. (1987). Assaying for superoxide dismutase activity: Some large consequences of minor changes in conditions. *Analytical Biochemistry*, *161*(2), 559–566. https://doi.org/10.1016/0003-2697(87)90489-1

Bilska, A., Dubiel, M., & Sokołowska-Jez, M. (2007). Alpha-lipoic acid differently affects the reserpine-induced oxidative stress in the striatum and prefrontal cortex of rat brain. *Elsevier*. https://www.sciencedirect.com/science/article/pii/S0306452207004605

Bonifácio, M. J., Archer, M., Rodrigues, M. L., Matias, P. M., Learmonth, D. A., Carrondo, M. A., & Soares-da-Silva, P. (2002). Kinetics and crystal structure of catechol-o-

methyltransferase complex with co-substrate and a novel inhibitor with potential therapeutic application. *Molecular Pharmacology*, *62*(4), 795–805.

Bowery, N., Bettler, B., & Froestl, W. (2002). International Union of Pharmacology. XXXIII. Mammalian γ-aminobutyric acidB receptors: structure and function. *EnnaPharmacological Reviews,*. https://pharmrev.aspetjournals.org/content/54/2/247.short

Broadhurst, P. L., & London. (1960). The place of animal psychology in the development of psychosomatic research. In *Adv. Psychosom. Med: Vol. I.*

Carlsson, & Carlsson, A. (1989). Marked locomotor stimulation in monoamine-depleted mice following treatment with atropine in combination with clonidine. *Journal of Neural Transmission - Parkinson's Disease and Dementia Section*, *1*(4), 317–322. https://doi.org/10.1007/BF02263486

Chalkha, M., Nour, H., Chebbac, K., Nakkabi, A., Bahsis, L., Bakhouch, M., Akhazzane, M., Bourass, M., Chtita, S., & Bin Jardan, Y. A. (2022). Synthesis, characterization, DFT mechanistic study, antimicrobial activity, molecular modeling, and ADMET properties of novel pyrazole-isoxazoline hybrids. *ACS Omega*, *7*(50), 46731–46744.

Chaudhuri, K. R., Healy, D. G., & Schapira, A. H. V. (2006). Non-motor symptoms of Parkinson's disease: diagnosis and management. *The Lancet Neurology*, *5*(3), 235–245. https://doi.org/10.1016/S1474-4422(06)70373-8

Chaumont, J., Guyon, N., Valera, A. M., Dugué, G. P., Popa, D., Marcaggi, P., Gautheron, V., Reibel-Foisset, S., Dieudonné, S., Stephan, A., Barrot, M., Cassel, J. C., Dupont, J. L., Doussau, F., Poulain, B., Selimi, F., Léna, C., & Isope, P. (2013). Clusters of cerebellar Purkinje cells control their afferent climbing fiber discharge. *Proceedings of the National Academy of Sciences of the United States of America*, *110*(40), 16223–16228. https://doi.org/10.1073/PNAS.1302310110

Chopade, P., Chopade, N., Zhao, Z., Mitragotri, S., Liao, R., & Chandran Suja, V. (2023). Alzheimer's and Parkinson's disease therapies in the clinic. *Bioengineering & Translational Medicine*, *8*(1), e10367.

Colombo, E., immunology, C. F.-T. in, & 2016, undefined. (n.d.). Astrocytes: key regulators of neuroinflammation. *Cell.ComE Colombo, C FarinaTrends in Immunology, 2016•cell.Com*. Retrieved September 14, 2023, from https://www.cell.com/trends/immunology/fulltext/S1471-4906(16)30072-2

Cordaro, M., Siracusa, R., Crupi, R., Impellizzeri, D., Peritore, A. F., D'Amico, R., Gugliandolo, E., Di Paola, R., & Cuzzocrea, S. (2018). 2-Pentadecyl-2-Oxazoline Reduces Neuroinflammatory Environment in the MPTP Model of Parkinson Disease. *Molecular Neurobiology*, *55*(12), 9251–9266. https://doi.org/10.1007/S12035-018-1064-2

da Silva Córneo, E., de Bem Silveira, G., Scussel, R., Correa, M. E. A. B., da Silva Abel, J., Luiz, G. P., Feuser, P. E., Silveira, P. C. L., & Machado-de-Ávila, R. A. (2020a). Effects of gold nanoparticles administration through behavioral and oxidative parameters in animal model of Parkinson's disease. *Colloids and Surfaces B: Biointerfaces*, *196*. https://doi.org/10.1016/j.colsurfb.2020.111302

da Silva Córneo, E., de Bem Silveira, G., Scussel, R., Correa, M. E. A. B., da Silva Abel, J., Luiz, G. P., Feuser, P. E., Silveira, P. C. L., & Machado-de-Ávila, R. A. (2020b). Effects of gold nanoparticles administration through behavioral and oxidative parameters in animal model of Parkinson's disease. *Colloids and Surfaces B: Biointerfaces*, *196*, 111302. https://doi.org/10.1016/J.COLSURFB.2020.111302

Daoui, O., Elkhattabi, S., & Chtita, S. (2022). Rational design of novel pyridine-based drugs candidates for lymphoma therapy. *Journal of Molecular Structure*, *1270*, 133964.

Darvesh, A. S., Carroll, R. T., Bishayee, A., Novotny, N. A., Geldenhuys, W. J., & Van Der Schyf, C. J. (2012). Curcumin and neurodegenerative diseases: A perspective. *Expert Opinion on Investigational Drugs*, *21*(8), 1123–1140. https://doi.org/10.1517/13543784.2012.693479

De Freitas, C. M., Busanello, A., Schaffer, L. F., Peroza, L. R., Krum, B. N., Leal, C. Q., Ceretta, A. P. C., Da Rocha, J. B. T., & Fachinetto, R. (2016). Behavioral and neurochemical effects induced by reserpine in mice. *Psychopharmacology*, *233*(3), 457–467. https://doi.org/10.1007/S00213-015-4118-4

De Zeeuw, C. I., & Berrebi, A. S. (1995). Postsynaptic Targets of Purkinje Cell Terminals in the Cerebellar and Vestibular Nuclei of the Rat. *European Journal of Neuroscience*, *7*(11), 2322–2333. https://doi.org/10.1111/J.1460-9568.1995.TB00653.X

Dhiman, S., Mannan, A., Taneja, A., Mohan, M., & Singh, T. G. (2024). Sirtuin dysregulation in Parkinson's disease: Implications of acetylation and deacetylation processes. *Life Sciences*, 122537.

Draoui, A., El Hiba, O., Abdelaati, E. K., Abbaoui, A., El Fari, R., Aitihya, M., & Gamrani, H. (2019). Differential impairment of short working and spatial memories in a rat model of progressive Parkinson's disease onset: A focus on the prodromal stage. *Brain Research Bulletin*, *150*, 307–316. https://doi.org/10.1016/j.brainresbull.2019.06.014

El-Shamarka, M. E. S., Abdel-Salam, O. M. E., Shafee, N., & Zeidan, H. M. (2022a). Curcumin modulation of L-dopa and rasagiline-induced neuroprotection in rotenone model of Parkinson's disease. *Iranian Journal of Basic Medical Sciences*, *26*(2), 139–147. https://doi.org/10.22038/IJBMS.2022.61687.13650

El-Shamarka, M. E. S., Abdel-Salam, O. M. E., Shafee, N., & Zeidan, H. M. (2022b). Curcumin modulation of L-dopa and rasagiline-induced neuroprotection in rotenone model of Parkinson's disease. *Iranian Journal of Basic Medical Sciences*, *26*(2), 139–147. https://doi.org/10.22038/IJBMS.2022.61687.13650

Fuentes, P., Paris, I., Nassif, M., Caviedes, P., & Segura-Aguilar, J. (2007). Inhibition of VMAT-2 and DT-diaphorase induce cell death in a substantia nigra-derived cell line - An experimental cell model for dopamine toxicity studies. *Chemical Research in Toxicology*, *20*(5), 776–783. https://doi.org/10.1021/TX600325U

Gao, H., Liu, B., Zhang, W., sciences, J. H.-T. in pharmacological, & 2003, undefined. (2003). Novel anti-inflammatory therapy for Parkinson's disease. *Cell.ComHM Gao, B Liu, W Zhang, JS HongTrends in Pharmacological Sciences, 2003•cell.Com*. https://doi.org/10.1016/S0165-6147(03)00176-7

Gao, H. M., Liu, B., Zhang, W., & Hong, J. S. (2003). Synergistic dopaminergic neurotoxicity of MPTP and inflammogen lipopolysaccharide: Relevance to the etiology of Parkinson's disease. *FASEB Journal*, *17*(13), 1–25. https://doi.org/10.1096/FJ.03-0203FJE

Ge, G., Sivasubramanian, B. P., Geng, B. D., Zhao, S., Zhou, Q., Huang, G., O'Connor, J. C., Clark, R. A., & Li, S. (2024). Long-term benefits of hematopoietic stem cell-based macrophage/microglia delivery of GDNF to the CNS in a mouse model of Parkinson's disease. *Gene Therapy*, 1–11.

Giri, R. K., Rajagopal, V., & Kalra, V. K. (2004). Curcumin, the active constituent of turmeric, inhibits amyloid peptide-induced cytochemokine gene expression and CCR5-mediated chemotaxis of THP-1 monocytes by modulating early growth response-1 transcription factor. *Journal of Neurochemistry*, *91*(5), 1199–1210. https://doi.org/10.1111/J.1471-4159.2004.02800.X

Goel, A., Kunnumakkara, A. B., & Aggarwal, B. B. (2008). Curcumin as "Curecumin": From kitchen to clinic. *Biochemical Pharmacology*, *75*(4). https://doi.org/10.1016/j.bcp.2007.08.016

Harrington, G. M. (1972). Strain differences in open-field behavior of the rat. *Psychonomic Science*, *27*(1), 51–53. https://doi.org/10.3758/BF03328887/METRICS

Hasan, W., Kori, R. K., Jain, J., Yadav, R. S., & Jat, D. (2020). Neuroprotective effects of mitochondria-targeted curcumin against rotenone-induced oxidative damage in cerebellum of mice. *Journal of Biochemical and Molecular Toxicology*, *34*(1), e22416. https://doi.org/10.1002/JBT.22416

Hassani, S., & Esmaeili, A. (2024). The neuroprotective effects of Ferulic acid in toxin-induced models of Parkinson's disease: a review. *Ageing Research Reviews*, 102299.

Heman, P., Barcia, C., Gómez, A., & Gómez, C. R. (2012). *Nigral degeneration correlates with persistent activation of cerebellar Purkinje cells in MPTP-treated monkeys*. https://repositori.uji.es/xmlui/handle/10234/72926

Iskusnykh, I. Y., Zakharova, A. A., Kryl'skii, E. D., & Popova, T. N. (2024). Aging, Neurodegenerative Disorders, and Cerebellum. *International Journal of Molecular Sciences*, *25*(2), 1018.

Juza, R., Musilek, K., Mezeiova, E., Soukup, O., & Korabecny, J. (2023). Recent advances in dopamine D2 receptor ligands in the treatment of neuropsychiatric disorders. *Medicinal Research Reviews*, *43*(1), 55–211.

Kabeer, A., Mailafiya, M., … A. D.-B. R., & 2019, undefined. (2019). Therapeutic potential of curcumin against lead-induced toxicity: A review. *Biomedpress.OrgA Kabeer, MM Mailafiya, A Danmaigoro, EA Rahim, MZA Bu BakarBiomedical Research and Therapy, 2019•biomedpress.Org*. http://home.biomedpress.org/index.php/BMRAT/article/view/528

Khadrawy, Y. A., Hosny, E. N., Magdy, M., & Mohammed, H. S. (2021). Antidepressant effects of curcumin-coated iron oxide nanoparticles in a rat model of depression. *European Journal of Pharmacology*, *908*. https://doi.org/10.1016/J.EJPHAR.2021.174384

Khadrawy, Y. A., Mourad, I. M., Mohammed, H. S., Noor, N. A., & Aboul Ezz, H. S. (2017). Cerebellar neurochemical and histopathological changes in rat model of Parkinson's disease induced by intrastriatal injection of rotenone. *Scholar.Cu.Edu.EgYA Khadrawy, IM Mourad, HS Mohammed, NA Noor, HS Aboul EzzGen. Physiol. Biophys, 2017•scholar.Cu.Edu.Eg*, *36*, 99–108. https://doi.org/10.4149/gpb_2016031

Kishi, S., Nagasu, H., Kidokoro, K., & Kashihara, N. (2024). Oxidative stress and the role of redox signalling in chronic kidney disease. *Nature Reviews Nephrology*, *20*(2), 101–119.

Leão, A. H. F. F., Sarmento-Silva, A. J., Santos, J. R., Ribeiro, A. M., & Silva, R. H. (2015a). Molecular, Neurochemical, and Behavioral Hallmarks of Reserpine as a Model for Parkinson's Disease: New Perspectives to a Long-Standing Model. *Brain Pathology*, *25*(4), 377–390. https://doi.org/10.1111/BPA.12253

Leão, A. H. F. F., Sarmento-Silva, A. J., Santos, J. R., Ribeiro, A. M., & Silva, R. H. (2015b). Molecular, Neurochemical, and Behavioral Hallmarks of Reserpine as a Model for Parkinson's Disease: New Perspectives to a Long-Standing Model. In *Brain Pathology* (Vol. 25, Issue 4, pp. 377–390). https://doi.org/10.1111/bpa.12253

Lobay, D. (2015). Rauwolfia in the Treatment of Hypertension. *Integrative Medicine: A Clinician's Journal*, *14*(3), 40. /pmc/articles/PMC4566472/

Lodha, R., & Bagga, A. (2000). Traditional Indian systems of medicine. *Europepmc.OrgR Lodha, A BaggaAnnals of the Academy of Medicine, Singapore, 2000•europepmc.Org*. https://europepmc.org/article/med/10748962

Lopatina, O., Yoshihara, T., Nishimura, T., Zhong, J., Akther, S., Fakhrul, A. A. K. M., Liang, M., Higashida, C., Sumi, K., Furuhara, K., Inahata, Y., Huang, J. J., Koizumi, K., Yokoyama, S., Tsuji, T., Petugina, Y., Sumarokov, A., Salmina, A. B., Hashida, K., … Higashida, H. (2014). Anxiety- and depression-like behavior in mice lacking the CD157/BST1 gene, a risk factor for Parkinson's disease. *Frontiers in Behavioral Neuroscience*, *8*(APR). https://doi.org/10.3389/FNBEH.2014.00133/FULL

Maheshwari, R., Singh, A., & Gaddipati, J. (2006). Multiple biological activities of curcumin: a short review. *Elsevier*. https://www.sciencedirect.com/science/article/pii/S0024320505012427

Mark, P., & Nilsson, L. (2001). Structure and dynamics of the TIP3P, SPC, and SPC/E water models at 298 K. *The Journal of Physical Chemistry A*, *105*(43), 9954–9960.

McGeer, P. L., & McGeer, E. G. (2008). Glial reactions in Parkinson's disease. *Movement Disorders*, *23*(4), 474–483. https://doi.org/10.1002/MDS.21751

Mohammed, H. S., Khadrawy, Y. A., El-Sherbini, T. M., & Amer, H. M. (2019). Electrocortical and Biochemical Evaluation of Antidepressant Efficacy of Formulated Nanocurcumin. *Applied Biochemistry and Biotechnology*, *187*(3), 1096–1112. https://doi.org/10.1007/S12010-018-2866-4

Monville, C., Torres, E. M., & Dunnett, S. B. (2006). Comparison of incremental and accelerating protocols of the rotarod test for the assessment of motor deficits in the 6-OHDA model. *Journal of Neuroscience Methods*, *158*(2), 219–223. https://doi.org/10.1016/j.jneumeth.2006.06.001

Morris, G. M., Huey, R., Lindstrom, W., Sanner, M. F., Belew, R. K., Goodsell, D. S., & Olson, A. J. (2009). AutoDock4 and AutoDockTools4: Automated docking with selective receptor flexibility. *Journal of Computational Chemistry*, *30*(16), 2785–2791.

Ojha, R. P., Rastogi, M., Devi, B. P., Agrawal, A., & Dubey, G. P. (2012). Neuroprotective effect of curcuminoids against inflammation-mediated dopaminergic neurodegeneration in the mptp model of parkinson's Disease. *Journal of Neuroimmune Pharmacology*, *7*(3), 609–618. https://doi.org/10.1007/s11481-012-9363-2

Orfali, R., Alwatban, A. Z., Orfali, R. S., Lau, L., Chea, N., Alotaibi, A. M., Nam, Y.-W., & Zhang, M. (2024). Oxidative stress and ion channels in neurodegenerative diseases. *Frontiers in Physiology*, *15*, 1320086.

Oukhrib, M., Tamegart, L., Assafi, A., Hejji, L., Azzouz, A., Villarejo, L. P., Haida, M., Mohamed, C., & Gamrani, H. (2023). Effects of graphene oxide nanoparticles administration against reserpine-induced neurobehavioral damage and oxidative stress in an animal model of Parkinson's disease. *Food and Chemical Toxicology*, *178*, 113904. https://doi.org/10.1016/J.FCT.2023.113904

Pasquini, J., Deuschl, G., Pecori, A., Salvadori, S., Ceravolo, R., & Pavese, N. (2023). The clinical profile of tremor in Parkinson's disease. *Movement Disorders Clinical Practice*, *10*(10), 1496–1506.

Paterniti, I., Campolo, M., Siracusa, R., Cordaro, M., Di Paola, R., Calabrese, V., Navarra, M., Cuzzocrea, S., & Esposito, E. (2017). Liver X receptors activation, through TO901317 binding, reduces neuroinflammation in Parkinson's disease. *PLoS ONE*, *12*(4). https://doi.org/10.1371/JOURNAL.PONE.0174470

Person, A., & Nature, I. R. (2012). Purkinje neuron synchrony elicits time-locked spiking in the cerebellar nuclei. *Nature.ComAL Person, IM RamanNature, 2012•nature.Com*. https://www.nature.com/articles/nature10732

Prajjwal, P., Kolanu, N. D., Reddy, Y. B., Ahmed, A., Marsool, M. D. M., Santoshi, K., Pattani, H. H., John, J., Chandrasekar, K. K., & Hussin, O. A. (2024). Association of Parkinson's disease to Parkinson's plus syndromes, Lewy body dementia, and Alzheimer's dementia. *Health Science Reports*, *7*(4), e2019.

Qamar, M. A., Tall, P., van Wamelen, D., Wan, Y. M., Rukavina, K., Fieldwalker, A., Matthew, D., Leta, V., Bannister, K., & Chaudhuri, K. R. (2024). Setting the clinical context to non-motor symptoms reflected by Park-pain, Park-sleep, and Park-autonomic subtypes of Parkinson's disease. In *International Review of Neurobiology* (Vol. 174, pp. 1–58). Elsevier.

Regoni, M., Valtorta, F., & Sassone, J. (2024). Dopaminergic neuronal death via necroptosis in Parkinson's disease: A review of the literature. *European Journal of Neuroscience*, *59*(6), 1079–1098.

Roos, K., Wu, C., Damm, W., Reboul, M., Stevenson, J. M., Lu, C., Dahlgren, M. K., Mondal, S., Chen, W., & Wang, L. (2019). OPLS3e: Extending force field coverage for drug-like small molecules. *Journal of Chemical Theory and Computation*, *15*(3), 1863–1874.

SRIMAL, R. C., & DHAWAN, B. N. (1973). Pharmacology of diferuloyl methane (curcumin), a non-steroidal anti-inflammatory agent. *Journal of Pharmacy and Pharmacology*, *25*(6), 447–452. https://doi.org/10.1111/J.2042-7158.1973.TB09131.X

Studio, D. (2016). Dassault Systemes BIOVIA. *Discovery Studio Modelling Environment, Release*, *4*.

Tamegart, L., Abbaoui, A., El khiat, A., Bouyatas, M. M., & Gamrani, H. (2021). Lead (Pb) exposure induces physiological alterations in the serotoninergic and vasopressin systems causing anxiogenic-like behavior in Meriones shawi: Assessment of BDMC as a neuroprotective compound for Pb-neurotoxicity and kidney damages. *Journal of Trace Elements in Medicine and Biology*, *65*. https://doi.org/10.1016/j.jtemb.2021.126722

Tamegart, L., Abbaoui, A., Oukhrib, M., Bouyatas, M. M., & Gamrani, H. (2021). Physiological Alterations of Subchronic Lead Exposure Induced Degeneration of Epithelial Cells in Proximal Tubules and the Remedial Effect of Curcumin-III in Meriones shawi: a Possible Link with Vasopressin Release. *Biological Trace Element Research*. https://doi.org/10.1007/s12011-021-02751-w

Tobinai, K., Shimoyama, M., … S. I.-J. J. of, & 1992, undefined. (1992). Phase I study of YK-176 (2′-deoxycoformycin) in patients with adult T-cell leukemia-lymphoma. *Academic.Oup.ComK Tobinai, M Shimoyama, S Inoue, S Takayasu, M Chikara, M Kozuru, S Oda, H NakajimaJapanese Journal of Clinical Oncology,*

1992•academic.Oup.Com. https://academic.oup.com/jjco/article-abstract/22/3/164/803428

Trott, O., & Olson, A. J. (2010). AutoDock Vina: improving the speed and accuracy of docking with a new scoring function, efficient optimization, and multithreading. *Journal of Computational Chemistry*, *31*(2), 455–461.

Turkez, H., Altay, O., Yildirim, S., Li, X., Yang, H., Bayram, C., Bolat, I., Oner, S., Tozlu, O. O., & Arslan, M. E. (2023). Combined metabolic activators improve metabolic functions in the animal models of neurodegenerative diseases. *Life Sciences*, *314*, 121325.

Uozumi, K., Hanada, S., Ohno, N., Ishitsuka, K., Shimotakahara, S., Otsuka, M., Chyuman, Y., Nakahara, K., Takeshita, T., Kuwazuru, Y., Saitov, T., Makino, T., Iwahashi, M., Utsunomiya, A., & Arima, T. (1995). Combination chemotherapy (RCM protocol: Response-oriented cyclic multidrug protocol) for the acute or lymphoma type adult t-cell leukemia. *Leukemia and Lymphoma*, *18*(3–4), 317–323. https://doi.org/10.3109/10428199509059624

Uusisaari, M., Neuroscience, T. K.-, & 2008, undefined. (2008). GABAergic synaptic communication in the GABAergic and non-GABAergic cells in the deep cerebellar nuclei. *Elsevier*. https://www.sciencedirect.com/science/article/pii/S0306452208011287

van Deijk, A. L. F., Camargo, N., Timmerman, J., Heistek, T., Brouwers, J. F., Mogavero, F., Mansvelder, H. D., Smit, A. B., & Verheijen, M. H. G. (2017). Astrocyte lipid metabolism is critical for synapse development and function in vivo. *Glia*, *65*(4), 670–682. https://doi.org/10.1002/GLIA.23120

Vergo, S., Johansen, J., Leist, M., research, J. L.-B., & 2007, undefined. (n.d.). Vesicular monoamine transporter 2 regulates the sensitivity of rat dopaminergic neurons to disturbed cytosolic dopamine levels. *Elsevier*. Retrieved October 12, 2023, from https://www.sciencedirect.com/science/article/pii/S0006899307022147

Volterra, A., Liaudet, N., & Savtchouk, I. (2014). Astrocyte Ca2+ signalling: an unexpected complexity. *Nature Reviews Neuroscience 2014 15:5*, *15*(5), 327–335. https://doi.org/10.1038/nrn3725

Voon, V., & Fox, S. H. (2007). Medication-Related Impulse Control and Repetitive Behaviors in Parkinson Disease. *Archives of Neurology*, *64*(8), 1089–1096. https://doi.org/10.1001/ARCHNEUR.64.8.1089

Voronkov, D. N., Khudoerkov, R. M., & Dovedova, E. L. (2013). Changes in neuroglial interactions in the cerebral nigrostriatal structures in a model of dopamine system dysfunction. *Zhurnal Nevrologii i Psihiatrii Imeni S.S. Korsakova*, *2013*(7).

Yamari, I., Abchir, O., Mali, S. N., Errougui, A., Talbi, M., El Kouali, M., & Chtita, S. (2023). The anti-SARS-CoV-2 activity of novel 9, 10-dihydrophenanthrene derivatives: an insight

into molecular docking, ADMET analysis, and molecular dynamics simulation. *Scientific African*, *21*, e01754.

Yamari, I., Abchir, O., Siddique, F., Zaki, H., Errougui, A., Talbi, M., Bouachrine, M., ElKouali, M., & Chtita, S. (2024). The anticoagulant potential of Lippia Alba extract in inhibiting SARS-CoV-2 Mpro: Density functional calculation, molecular docking analysis, and molecular dynamics simulations. *Scientific African*, *23*, e01986.

Zorec, R., Verkhratsky, A., Rodríguez, J. J., & Parpura, V. (2016). Astrocytic vesicles and gliotransmitters: Slowness of vesicular release and synaptobrevin2-laden vesicle nanoarchitecture. *Neuroscience*, *323*, 67–75. https://doi.org/10.1016/J.NEUROSCIENCE.2015.02.033

Figure captions

Fig. 1: Schematic representation of the experimental design. Administration of the various treatments, behavioural tests, euthanasia, biochemical and enzymatic analyses and histological and immunohistochemical analyses.

Fig. 2: Effect of CUR, Madopar or both on motor coordination (2A) and spontaneous motor activity (2B) in mice treated with RES. Motor coordination and spontaneous motor activity were measured for 5 min as described in the text. Values are expressed as mean ±SEM. *P<0.05 compared with control group, #P<0.05 compared with RES-treated group.

Fig. 3: Effects of CUR and Madopar or both on MDA (3A) and SOD (3B) levels in the cerebellum after treatment with RES. Data are expressed as mean ± SEM. *P<0.05 vs control, #P<0.05 vs RES alone.

Fig. 4: Representative photomicrographs of histological sections of the cerebellum stained with HE in the different groups: (A) Control, (B) RES alone, (C) RES+CUR, (D) RES+MAD, (E) RES+CUR+MAD and (F) Representative histogram of the rate of Purkinje cell degeneration where the data are expressed as a percentage (%) of normal and degenerated cells. *P<0.05 compared with the control group, #P<0.05 compared with the group treated with RES alone.

Fig. 5: Effects of CUR, Madopar or both on astrocyte density and morphology in the cerebellum after treatment with RES, revealed by GFAP immunostaining. (A) Control, (B) RES alone, (C) RES+CUR, (D) RES+MAD and (E) RES+CUR+MAD. Data are expressed as mean ± SEM. *P<0.05 compared with the control group, #P<0.05 compared with the group treated with RES alone.

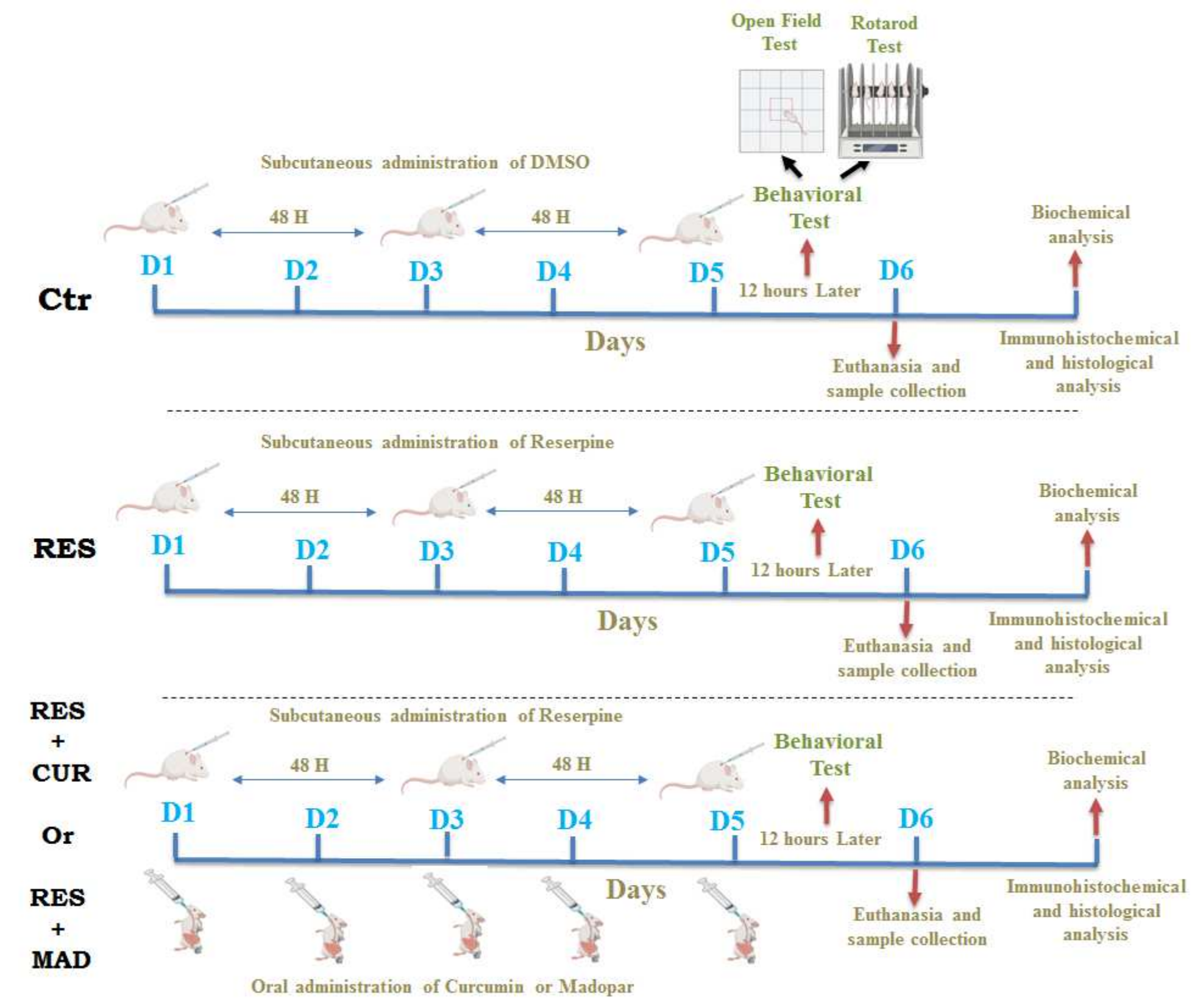
Fig. 6: 2D representation of COMT-ligand interactions (a) Cur, and (b) the Madopar used as reference drug.

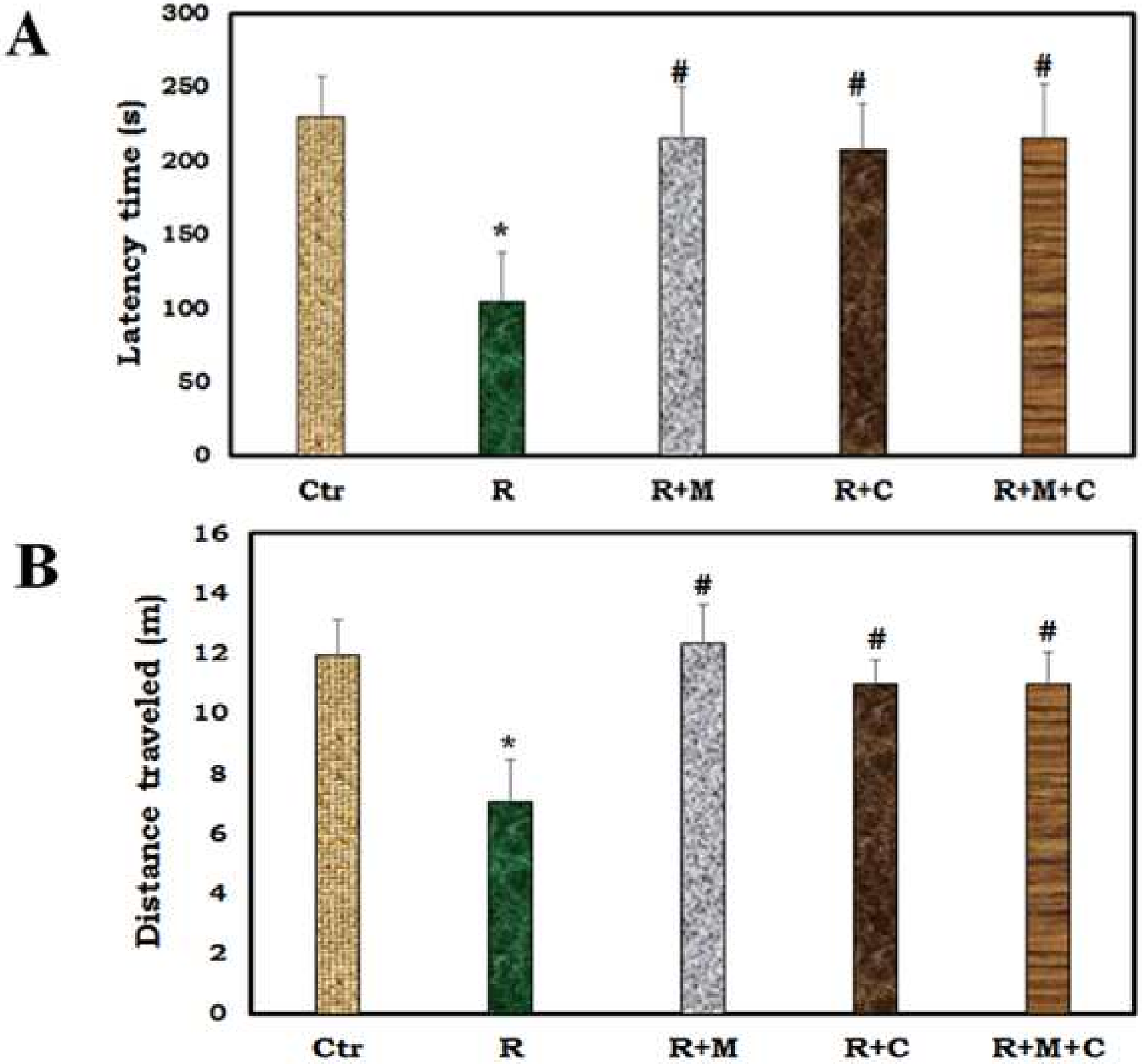
Fig. 7: The root means square deviation (RMSD) of COMT-Curcumin (a) and COMT-Madopar (b) over the MD of 100 ns.

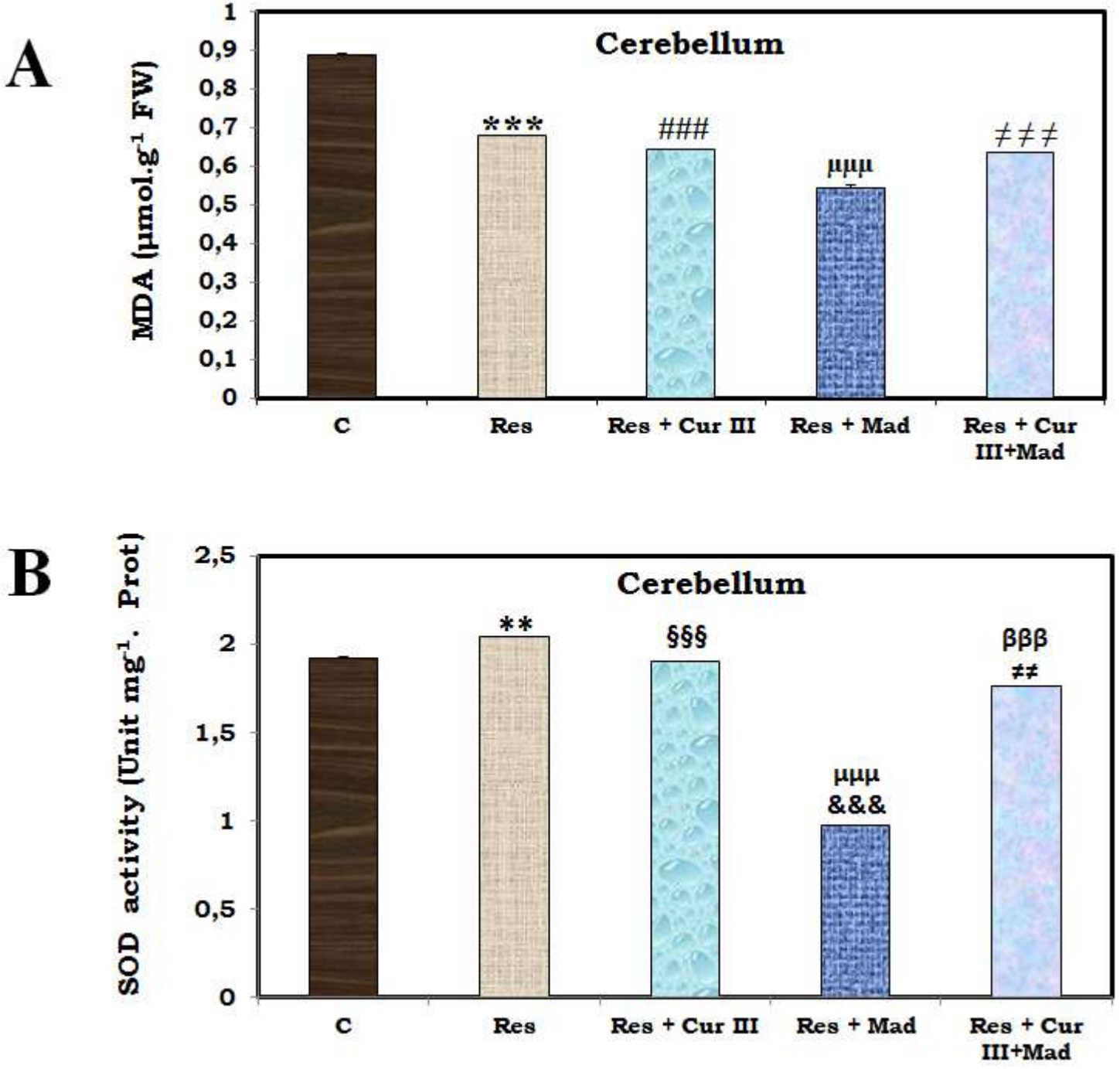
Fig. 8: The RMSF of COMT-Curcumin (a) and COMT-Madopar, over the MD of 100 ns.

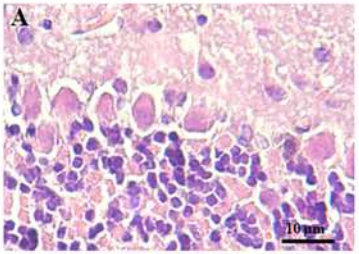
Fig. 9: Simulation interaction plots and histograms of Curcumin (a), Madopar (b) in complex with protein COMT.

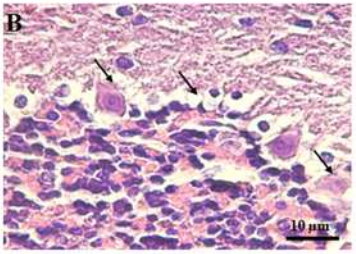
Fig. 10: Evolution of RMSD, Rg, MolSA, SASA, PSA during 100 ns, for Curcumin (a), Madopar (b).

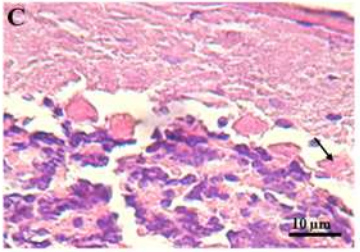

Open Field Test
Rotarod Test
Subcutaneous administration of DMSO
48 H
48 H
Behavioral Test
Biochemical analysis
D1
D2
D3
D4
D5
12 hours Later
D6
Ctr
Days
Euthanasia and sample collection
Immunohistochemical and histological analysis
Subcutaneous administration of Reserpine
48 H
48 H
Behavioral Test
Biochemical analysis
RES
D1
D2
D3
D4
D5
12 hours Later
D6
Days
Euthanasia and sample collection
Immunohistochemical and histological analysis
RES + CUR Or RES + MAD
Subcutaneous administration of Reserpine
48 H
48 H
Behavioral Test
Biochemical analysis
D1
D2
D3
D4
D5
12 hours Later
D6
Days
Euthanasia and sample collection
Immunohistochemical and histological analysis
Oral administration of Curcumin or Madopar

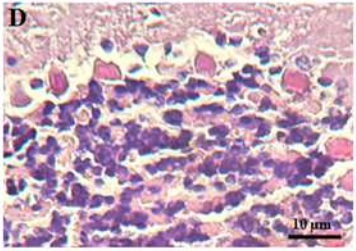

A
Latency time (s)
300
250
200
150
100
50
0
*
#
#
#
Ctr
R
R+M
R+C
R+M+C
B
Distance traveled (m)
16
14
12
10
8
6
4
2
0
*
#
#
#
Ctr
R
R+M
R+C
R+M+C

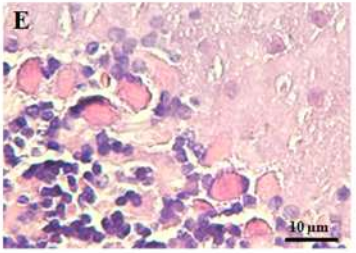

A
Cerebellum
MDA (µmol.g-1 FW)
1
0,9
0,8
0,7
0,6
0,5
0,4
0,3
0,2
0,1
0
***
###
µµµ
≠≠≠
C
Res
Res + Cur III
Res + Mad
Res + Cur III+Mad
B
Cerebellum
SOD activity (Unit mg-1. Prot)
2,5
2
1,5
1
0,5
0
**
§§§
µµµ
&&&
βββ
≠≠
C
Res
Res + Cur III
Res + Mad
Res + Cur III+Mad

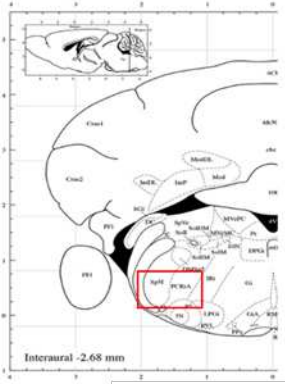

A
10 µm


B
10 µm

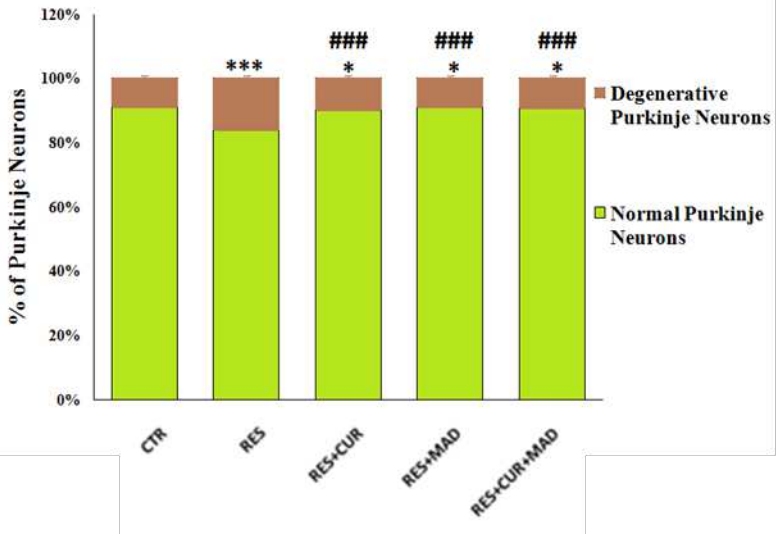

C
10 µm

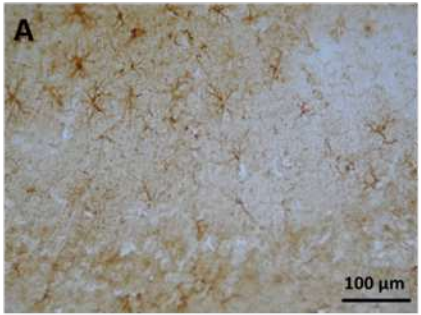

D
10 µm

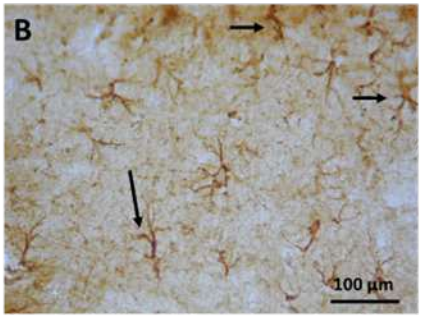

E
10 µm

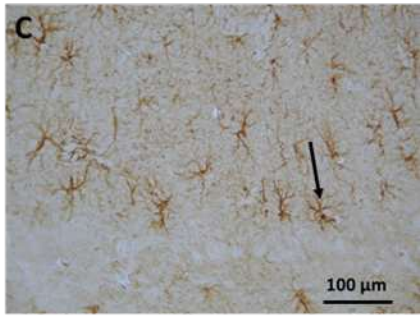

Interaural -2.68 mm

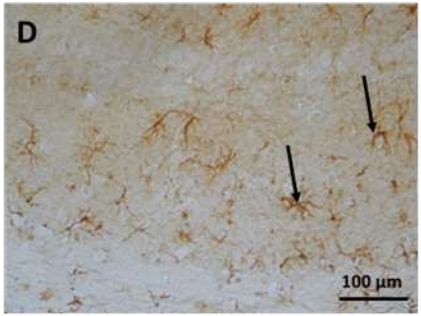
F

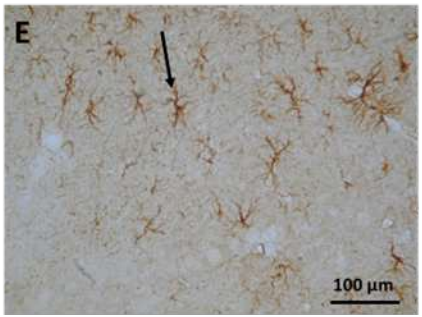

120%
100%
80%
60%
40%
20%
0%
% of Purkinje Neurons
***
###
*
###
*
###
*
Degenerative Purkinje Neurons
Normal Purkinje Neurons
CTR
RES
RES+CUR
RES+MAD
RES+CUR+MAD

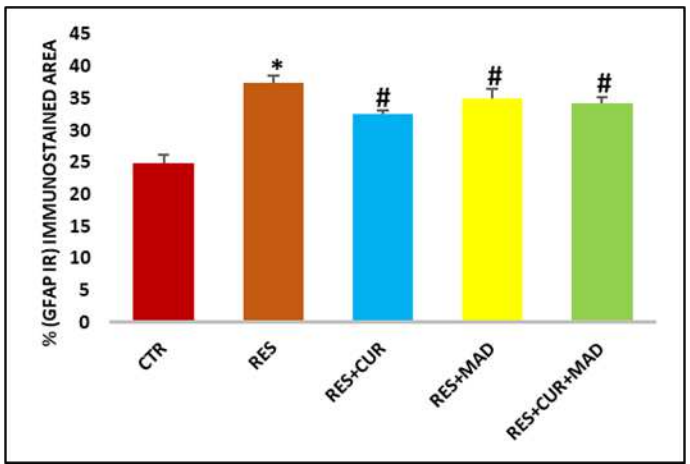

A
100 µm

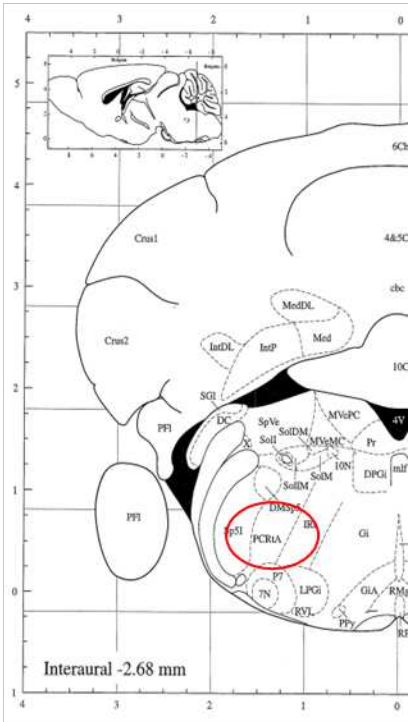

B
100 µm

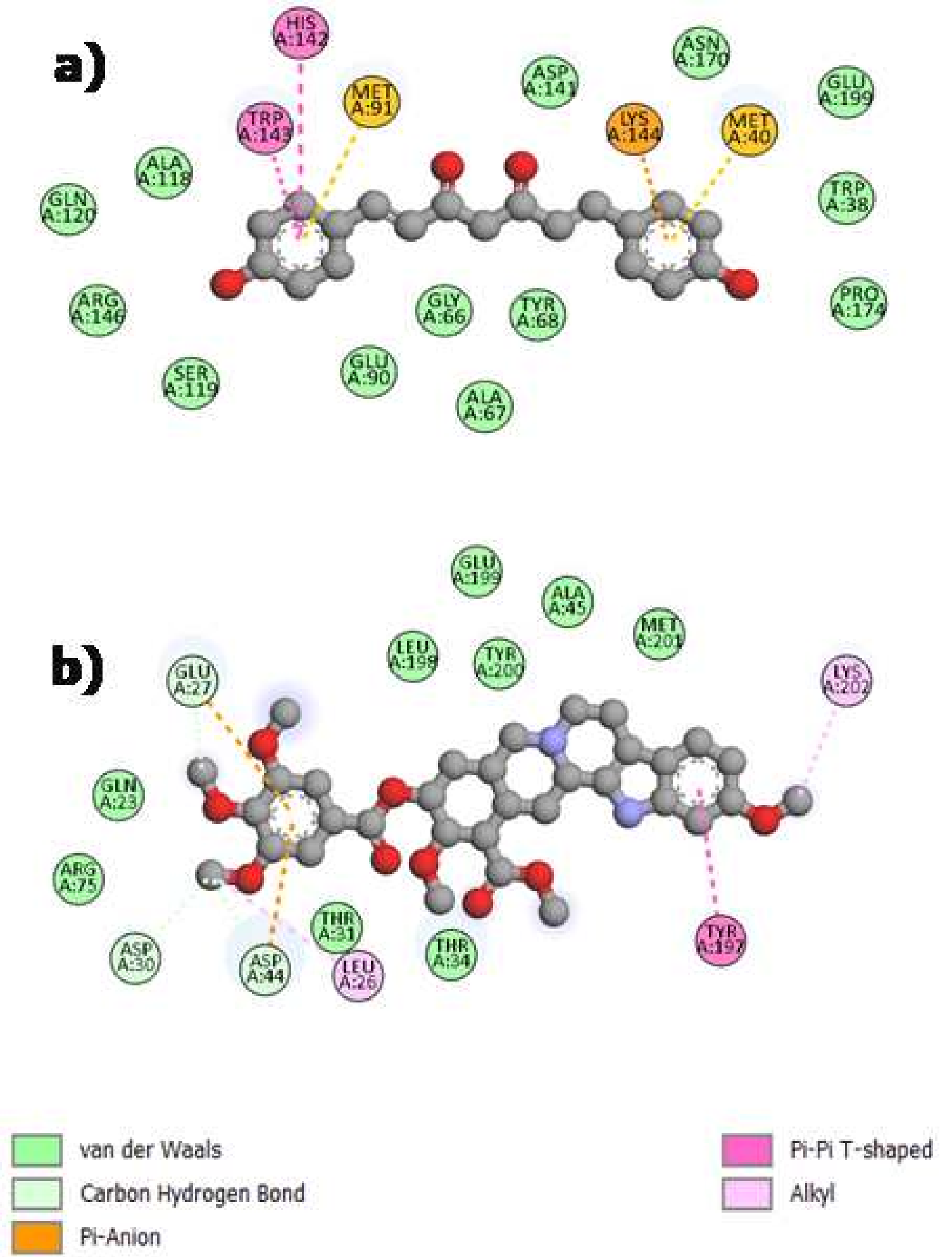

C
100 µm

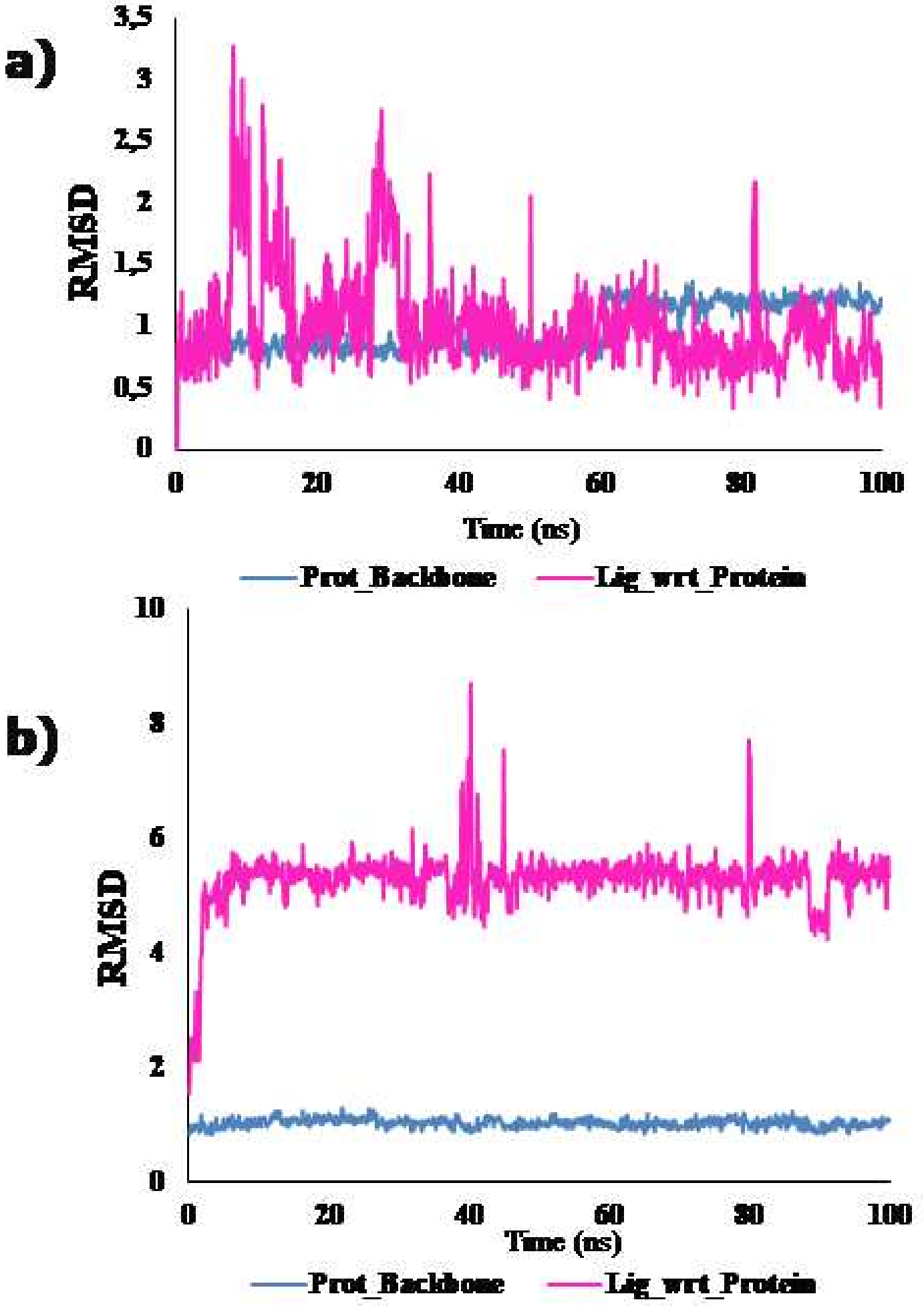

D
100 µm

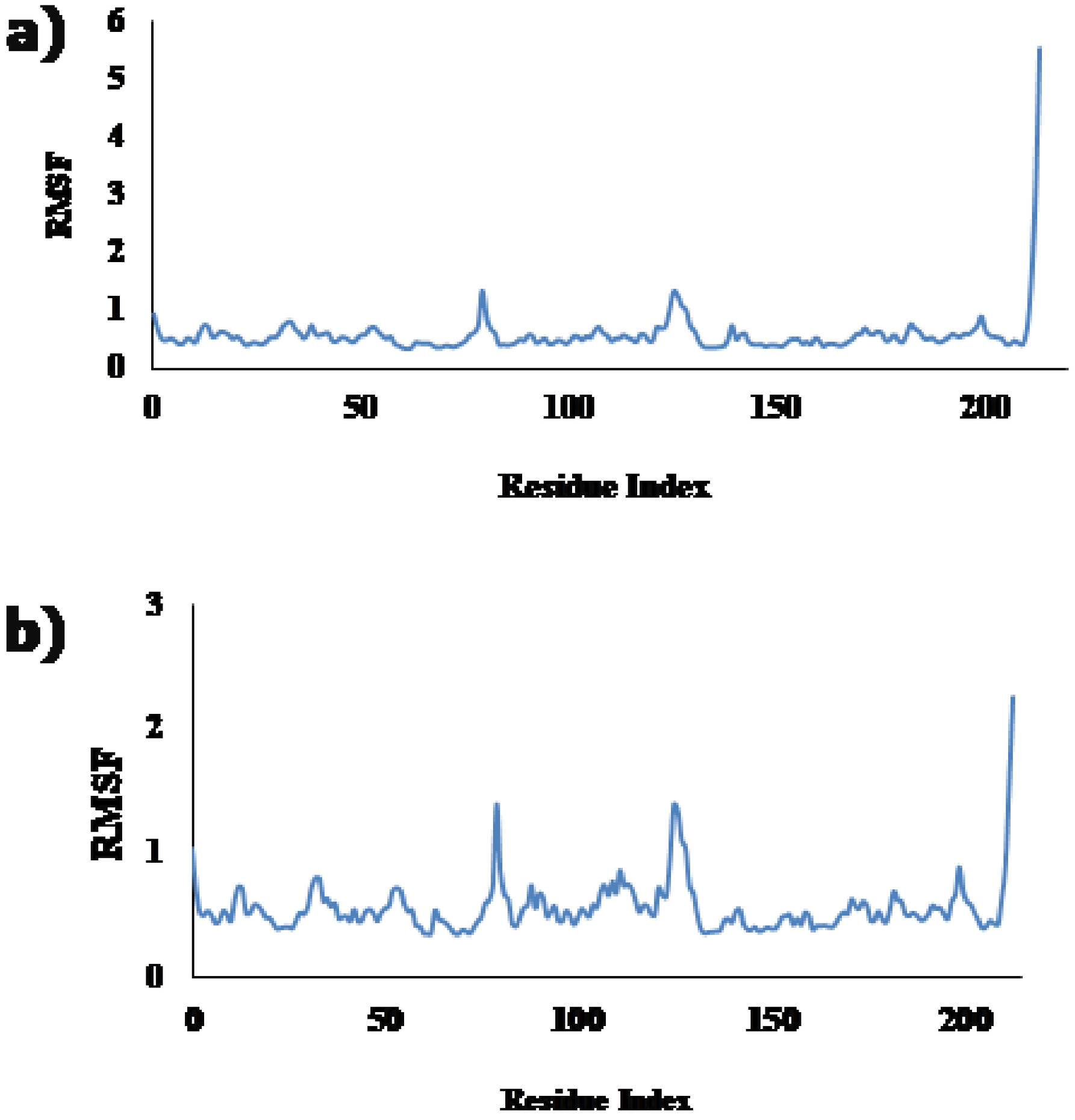

E
100 µm

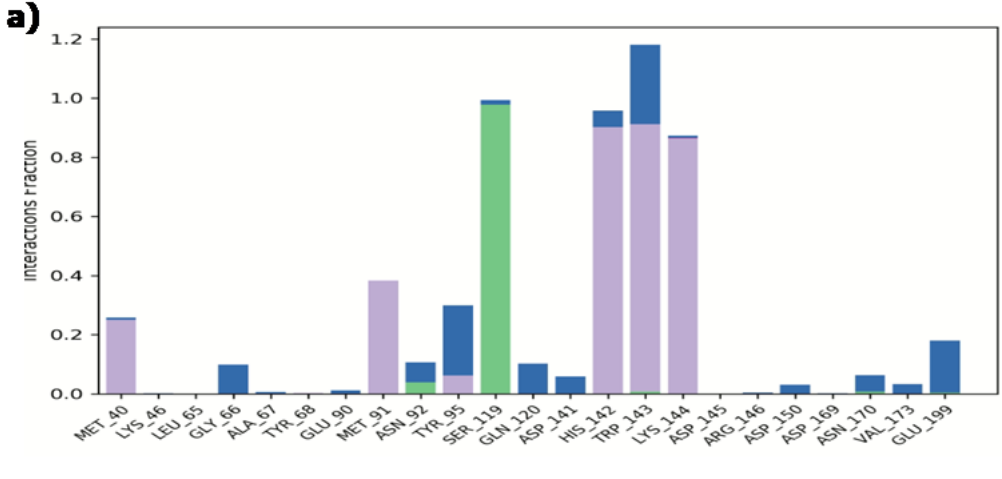

% (GFAP IR) IMMUNOSTAINED AREA
45
40
35
30
25
20
15
10
5
0
*
#
#
#
CTR
RES
RES+CUR
RES+MAD
RES+CUR+MAD

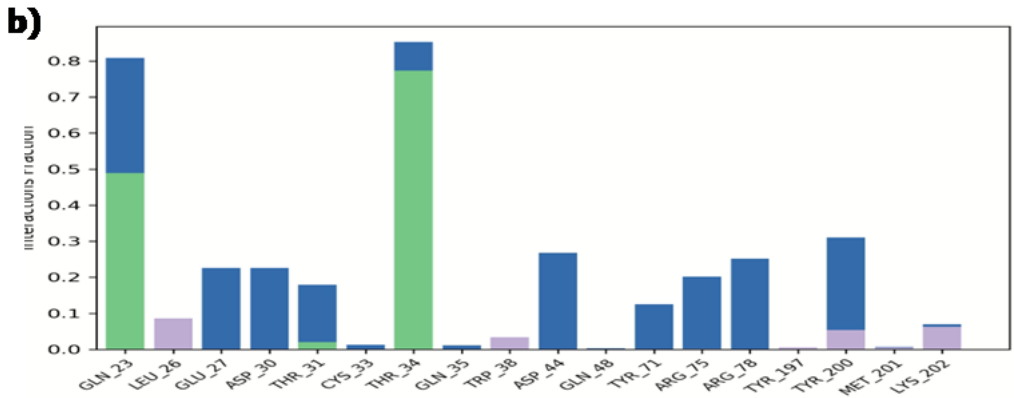

Crus1
Crus2
MedDL
IntDL
IntP
Med
SCl
DC
SpVe
SolDM
SolI
MVePC
MVeMC
SolM
SolIM
I6N
DPGi
PFl
DMS
IRt
PCRtA
Gi
7N
LPGi
RVL
GiA
Interaural -2.68 mm

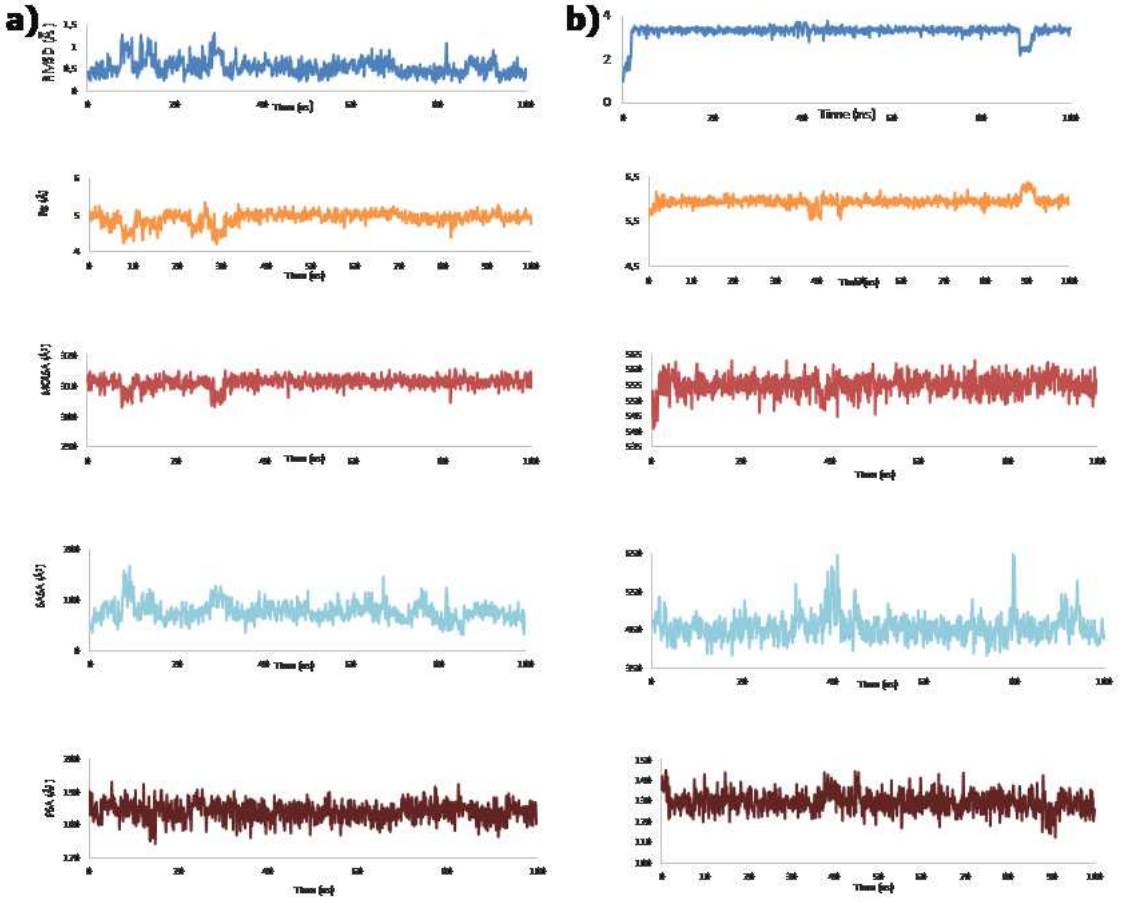

a)
HIS A:142
MET A:91
TRP A:143
ALA A:118
GLN A:120
ARG A:146
SER A:119
GLU A:90
ALA A:67
GLY A:66
TYR A:68
ASP A:141
ASN A:170
LYS A:144
MET A:40
GLU A:199
TRP A:38
PRO A:174
b)
GLU A:199
ALA A:45
MET A:201
LEU A:199
TYR A:200
GLU A:27
LYS A:202
GLN A:23
ARG A:75
ASP A:30
ASP A:44
THR A:31
LEU A:26
THR A:34
TYR A:197
van der Waals
Carbon Hydrogen Bond
Pi-Anion
Pi-Pi T-shaped
Alkyl

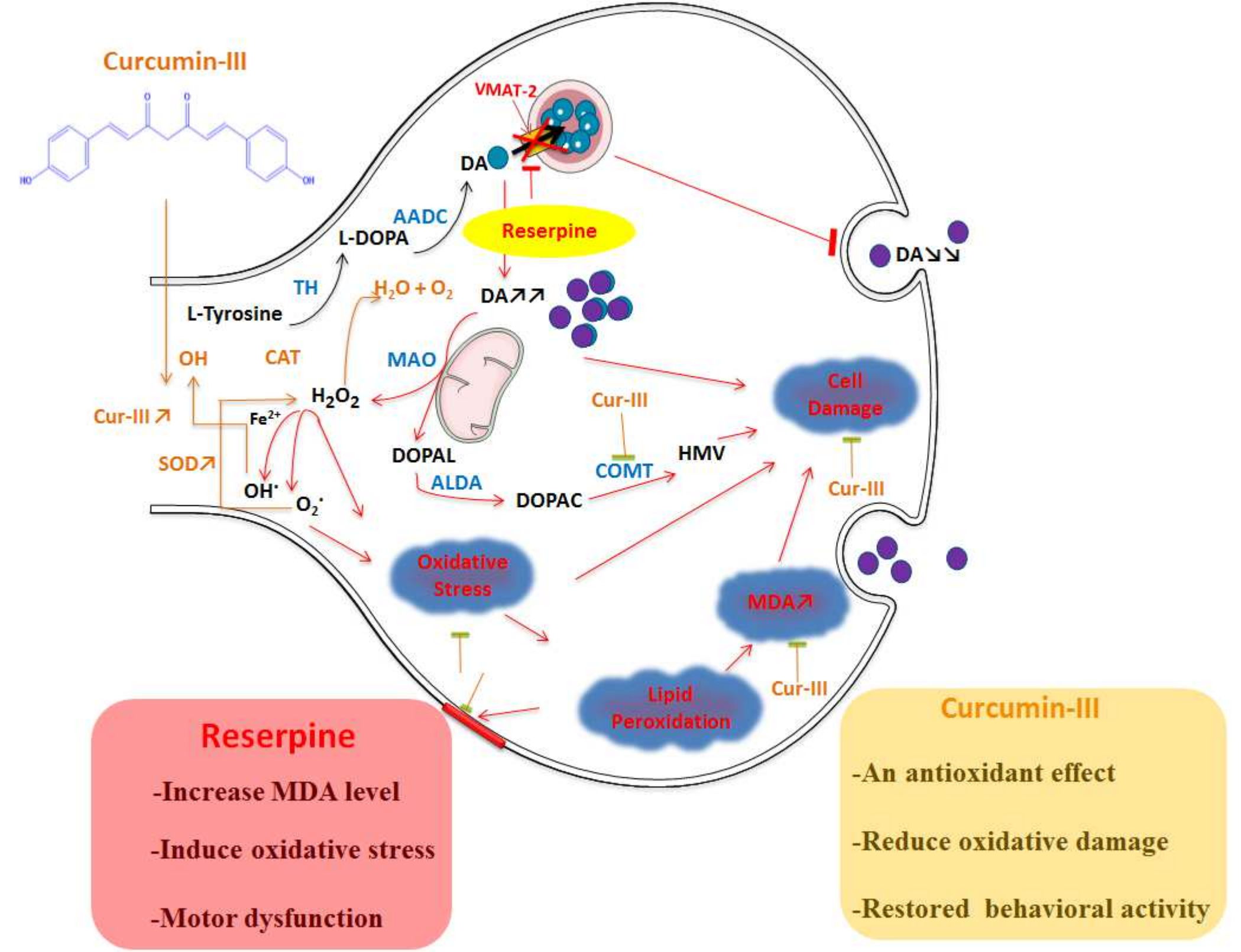

a)
RMSD
3,5
3
2,5
2
1,5
1
0,5
0
0
20
40
60
80
100
Time (ns)
Prot_Backbone
Lig_wrt_Protein
b)
RMSD
10
8
6
4
2
0
0
20
40
60
80
100
Time (ns)
Prot_Backbone
Lig_wrt_Protein


a)
RMSF
6
5
4
3
2
1
0
0
50
100
150
200
Residue Index
b)
RMSF
3
2
1
0
0
50
100
150
200
Residue Index


a)
Interactions fraction
1.2
1.0
0.8
0.6
0.4
0.2
0.0
MET_40
LYS_46
LEU_65
GLY_66
ALA_67
TYR_68
GLU_90
MET_91
ASN_92
TYR_95
SER_119
GLN_120
ASP_141
HIS_142
TRP_143
LYS_144
ASP_145
ARG_146
ASP_150
ASP_169
ASN_170
VAL_173
GLU_199


b)
0.8
0.7
0.6
0.5
0.4
0.3
0.2
0.1
0.0
GLN_23
LEU_26
GLU_27
ASP_30
THR_31
CYS_33
THR_34
GLN_35
TRP_38
ASP_44
GLN_48
TYR_71
ARG_75
ARG_78
TYR_197
TYR_200
MET_201
LYS_202


a)
b)
Time (sec)
Time (ms)


Curcumin-III
VMAT-2
DA
AADC
L-DOPA
Reserpine
DA↘↘
TH
L-Tyrosine
$H_2O + O_2$
DA↗↗
OH
CAT
MAO
Cell Damage
Cur-III
H_2O_2
Cur-III↗
Fe^{2+}
SOD↗
DOPAL
COMT
HMV
ALDA
$OH^{\cdot}$
$O_2^{\cdot}$
DOPAC
Cur-III
Oxidative Stress
MDA↗
Lipid Peroxidation
Cur-III
Reserpine
-Increase MDA level
-Induce oxidative stress
-Motor dysfunction
Curcumin-III
-An antioxidant effect
-Reduce oxidative damage
-Restored behavioral activity